

American University in Cairo

## AUC Knowledge Fountain

---

Theses and Dissertations

---

6-1-2016

### Gold nanoparticles-based sensors for detection of mycobacterium tuberculosis genomic DNA

Amira Hazem Mansour

Follow this and additional works at: <https://fount.aucegypt.edu/etds>

---

#### Recommended Citation

##### APA Citation

Mansour, A. (2016). *Gold nanoparticles-based sensors for detection of mycobacterium tuberculosis genomic DNA* [Master's thesis, the American University in Cairo]. AUC Knowledge Fountain.

<https://fount.aucegypt.edu/etds/227>

##### MLA Citation

Mansour, Amira Hazem. *Gold nanoparticles-based sensors for detection of mycobacterium tuberculosis genomic DNA*. 2016. American University in Cairo, Master's thesis. *AUC Knowledge Fountain*.

<https://fount.aucegypt.edu/etds/227>

This Thesis is brought to you for free and open access by AUC Knowledge Fountain. It has been accepted for inclusion in Theses and Dissertations by an authorized administrator of AUC Knowledge Fountain. For more information, please contact [mark.muehlhaeusler@aucegypt.edu](mailto:mark.muehlhaeusler@aucegypt.edu).



School of Sciences and Engineering

**Gold Nanoparticles-Based Sensors for Detection of *Mycobacterium tuberculosis*  
genomic DNA**

A Thesis Submitted to  
The Nanotechnology Master's Program  
In partial fulfillment of the requirements for  
The degree of Master of Science

By:

**Amira Hazem Mohamed Mansour**

Under the supervision of:

**Prof. Dr. Hassan M.E. Azzazy** (Advisor)

Department of Chemistry, The American University in Cairo, Egypt

Fall 2015

The American University in Cairo

**Gold Nanoparticles-Based Sensors for Detection of *Mycobacterium tuberculosis*.  
genomic DNA**

Thesis Submitted by

**Amira Hazem Mohamed Mansour**

To the Nanotechnology Graduate Program

Fall 2015

In partial fulfillment of the requirements form  
The degree of Master of Science in Nanotechnology

Has been approved by

Thesis Committee Chair and Thesis Supervisor: Prof. Dr. Hassan M.E. Azzazy

Affiliation: Professor of Chemistry, School of Sciences and Engineering, The  
American University in Cairo.

Thesis Committee Internal Examiner: Dr. Tarek Madkour

Affiliation: Professor of Polymer Chemistry, School of Sciences and Engineering,  
The American University in Cairo.

Thesis Committee External Examine: Dr. Khaled Abou Aisha

Affiliation: Professor of microbiology and immunology, Department of Microbiology  
and Immunology, The German University in Cairo

Thesis Committee Moderator: Dr. Nageh Allam

Affiliation: Associate Professor of physics, School of Sciences and Engineering, The  
American University in Cairo.

---

Dept. Chair/Director Date Dean Date

## ACKNOWLEDGEMENTS

I would like to express my immense gratitude to Prof. Dr. Hassan Azzazy, my advisor. I thank him for the knowledge, learning opportunities and scientific support. And now I am very proud to call myself his student and I will be in his debt forever.

I also thank the team of the novel diagnostics and therapeutic research (established by Prof. Dr. Hassan Azzazy) for their support, advice and encouragement. They have always supportive and helpful. I thank Mahmoud Khalil and Salma Tamam for their great help.

I thank Dr. Azza Hegazy, Director of the Central Labs, Ministry of health, for allowing me to take the needed clinical samples and providing their demographic data.

And finally I thank all my family. I have been blessed by GOD to have such an encouraging and motivating family. I appreciate their support and patience.

Finally I thank my God's gift; my daughter Lara. She is always my spark that lights up my life and inspires me to expend my effort that may be one day, she benefits from this effort.

## ABSTRACT

The American University in Cairo

### **Gold Nanoparticles-Based Sensors for Detection of *Mycobacterium tuberculosis* Genomic DNA**

By: Amira Hazem Mohamed Mansour

Under the supervision of Prof. Dr. Hassan M.E. Azzazy

Tuberculosis (TB) caused by *Mycobacterium tuberculosis* (MTB), is an airborne disease that strikes one third of the globe's population. In addition to infection of 9.6 million patients, TB claimed the lives of 1.5 million people in 2014 only. The majority of TB patients are present in the third world where the balance between cost-effective diagnostic method and prevalence of TB is difficult to achieve. Accurate diagnosis of TB is necessary to timely initiation of treatment. The available diagnostic tools are slow, while the rapid methods are either inaccurate or relatively unaffordable. So, sometimes the diagnosis is presumptive based on the clinical findings and the treatment is empiric. The treatment is lengthy and demands the administration of multiple antibiotics. However, the emergence of drug resistance threatened the global control programs of TB.

The objective of this work is to develop cheap, fast and accurate detection methods. Two gold nanoparticles (AuNPs) based sensors were developed for colorimetric and fluorometric detection of MTB. Seventy two anonymous sputum samples were cultured then DNA was extracted. MTB H37Ra was the positive control while *M. smegmatis* and 8 non-MTB and negative controls. Characterization of the samples was achieved by multiplex PCR using MTB and NTM specific primers. Random samples were amplified by 16S-23S ITS primers and sequenced. Drug resistance associated mutations of MDR-TB were identified by MAS-PCR.

The colorimetric assay aim was the detection of amplified MTB DNA by cationic AuNPs. The samples were amplified by *IS6110* and *rpoB* primers. Only MTB samples yielded amplicons. So the negatively charged dsDNA attracted the positively charged AuNPs inducing their aggregation and the color turned blue. While the

negative samples did not yield any amplicons and the AuNPs remained dispersed so the color was red. The sensitivity and specificity was 100% and the detection limit was 5.4 ng/μl of MTB DNA.

The fluorometric assay exploited the quenching property of 40 nm AuNPs. The unamplified DNA was fragmented in the presence of 16s rDNA specific probe tagged with the fluorophore CY-3 by sonication and denatured for 3 min at 95 °C followed by annealing at 52°C for 45 sec. Then AuNPs were added and the fluorescence was measured. By FRET, the relative fluorescence was calculated revealing a cut-off value of 3. In MTB samples, the CY3-16s rDNA specific probe hybridized with its target and became spaced from the AuNPs allowing high fluorescence to be detected. Due to the lack of target-probe hybridization in the negative samples, the AuNPs were adsorbed on the probe and thus the fluorescence is quenched. Thirteen samples were chosen randomly, amplified and sequenced. Sequencing confirmed that 12/13 samples were MTB with 100% concordance with the multiplex PCR and FRET. The assay had sensitivity and specificity of 98.6% and 90% respectively and concordance of 98% with multiplex PCR. The detection limited was calculated to be 10 ng/ul. In conclusion, two AuNPs based sensors were developed to allow low cost and rapid detection of MTB on low source settings. The assays are rapid, sensitive and can have great potential in clinical practice for TB diagnosis.

## Table of Contents

LIST OF TABLES.....	ix
LIST OF FIGURES.....	x
LIST OF ABBREVIATIONS.....	xii
Chapter 1. Introduction and literature review.....	1
1.1. History of Tuberculosis (TB).....	1
1.2. Tuberculosis.....	1
1.3. <i>Mycobacterium tuberculosis</i> .....	1
1.4. Pathophysiology of TB.....	2
1.5. TB Vaccine.....	3
1.6. TB treatment.....	3
1.6.1. First line antibiotics.....	4
1.6.2. Second line antibiotics.....	5
1.7. TB diagnosis.....	5
1.7.1. Specimens collection and preservation.....	6
1.7.2. Microscopic observation.....	7
1.7.3. Digital chest X-ray.....	8
1.7.4. Biomarkers-based MTB detection.....	8
1.7.4.1. Chromatographic detection of MTB.....	8
1.7.4.2. VOC for detection of MTB.....	8
1.7.5. Immuno-response-based assays.....	9
1.7.5.1. Tuberculin test.....	9
1.7.5.2. Serological assays.....	9
1.7.6. Bacterial culture.....	9
1.7.7. Nucleic Acids Amplification Techniques (NAATs).....	11
1.7.7.1. Automated MTB detection assays.....	13
1.7.7.2. Autonomous MTB detection assays.....	14
1.7.7.3. Line probe assays.....	14
1.7.7.4. DNA microarrays.....	14
1.7.7.5. Modular, cartridge-based, fully automated NAATs.....	15
1.7.7.6. Semi-automated NAATs.....	15
1.7.8. Detection of TB by phage-display.....	16

1.7.9. Detection of TB by nanoparticles.....	16
1.7.9.1. Gold nanoparticles (AuNPs).....	16
1.7.9.1.1. AuNPs synthesis.....	17
1.7.9.1.2. Modified AuNPs for MTB detection.....	18
1.7.9.1.3. Unmodified AuNPs for MTB detection.....	19
1.7.9.2. Detection of TB by FRET.....	19
1.8. Thesis scope and objectives.....	21
Chapter 2. Materials and Methods.....	22
2.1. Clinical bacterial strains.....	22
2.2. DNA extraction.....	22
2.3. Identification of the bacterial strains by PCR.....	23
2.3.1. Species differentiation using multiplex PCR.....	23
2.3.2. Amplification of 16S-23S ITS and Sequencing.....	23
2.3.3. Identification of drug resistance mutations of MDR-TB by MAS PCR.....	24
2.4. AuNPs-based sensors for MTB DNA detection.....	24
2.4.1. Cationic AuNPs-based sensor.....	24
2.4.1.1. Cationic AuNPs synthesis.....	24
2.4.1.2. Amplification of MTB DNA by <i>IS6110</i> primers.....	25
2.4.1.3. Amplification of MTB DNA by <i>rpoB</i> primers.....	25
2.4.1.4. Cationic AuNPs assay.....	25
2.4.1.5. Detection limit for cationic AuNPs assay.....	25
2.4.2. AuNPs-based FRET sensor for detection of MTB.....	26
2.4.2.1. Anionic AuNPs synthesis.....	26
2.4.2.2. Probe sequence.....	26
2.4.2.3. Optimization of the FRET assay.....	26
2.4.2.4. Detection of MTB DNA using FRET assay.....	26
2.4.2.5. Detection limit of FRET assay.....	27
2.5. Data interpretation and statistical analysis.....	27
Chapter 3. Results.....	28
3.1. Clinical bacterial strains.....	28
3.2. Characterization of the bacterial strains by PCR.....	28
3.2.1. Species differentiation by multiplex PCR.....	28
3.2.2. Amplification of 16S-23S (ITS) and Sequencing.....	28
3.2.3. Identification of drug resistance mutations of MDR-TB by MAS- PCR.....	29
3.3. AuNPs-based sensors for MTB DNA detection.....	29



<b>3.3.1. AuNPs Characterization.....</b>	<b>30</b>
<b>3.3.2. Cationic AuNPs-based sensor .....</b>	<b>29</b>
<b>3.3.2.1. <i>IS6110</i> amplification of MTB DNA.....</b>	<b>29</b>
<b>3.3.2.2. <i>rpoB</i> amplification of MTB DNA.....</b>	<b>30</b>
<b>3.3.2.3. Cationic AuNPs assay and detection limit.....</b>	<b>30</b>
<b>3.3.3. AuNPs-based FRET assay for MTB DNA detection.....</b>	<b>30</b>
<b>3.3.3.1. Optimization of FRET assay and investigation of the clinical bacterial strains by FRET.....</b>	<b>30</b>
<b>3.3.3.2. Detection limit by FRET.....</b>	<b>31</b>
<b>Chapter 4. Discussion.....</b>	<b>32</b>
<b>Chapter 5. Conclusion and Future Perspectives.....</b>	<b>36</b>
<b>6- Tables.....</b>	<b>37</b>
<b>7- Figures.....</b>	<b>54</b>
<b>8- References.....</b>	<b>84</b>

## LIST OF TABLES

<b>Table 1.</b> First line antibiotics, their mode of action and their main adverse effects	<b>38</b>
<b>Table 2.</b> Genes of the common mutation(s) in the resistant strains, normal role of the gene, the frequency, the mutation site and the effect of the associated mutations	<b>39</b>
<b>Table 3.</b> Comparison between the most applicable diagnostic approaches of TB	<b>40</b>
<b>Table 4.</b> The commercially available NAATs for MTB detection	<b>41</b>
<b>Table 5.</b> Pipeline of the development of NAATs for MTB detection	<b>42</b>
<b>Table 6.</b> WHO recommendation about the role of NAATs in TB diagnosis	<b>45</b>
<b>Table 7.</b> Comparison between the main diagnostic assays for detection of MTB by AuNPs	<b>46</b>
<b>Table 8.</b> Assays developed for the detection of MTB by FRET	<b>48</b>
<b>Table 9.</b> The primers and amplicons sizes used to differentiate MTB from NTM	<b>49</b>
<b>Table 10.</b> Samples chosen randomly and their sequencing results	<b>50</b>
<b>Table 11.</b> The primers used for identification of drug resistance associated mutations	<b>51</b>
<b>Table 12.</b> Amplicons size by MAS PCR	<b>52</b>
<b>Table 13.</b> Optimizing the amount of the AuNPs for the optimum quenching	<b>53</b>
<b>Table 14.</b> Detection limit of FRET assay	<b>54</b>

## LIST OF FIGURES

<b>Figure 1.</b> Top causes of deaths worldwide for 2014	<b>55</b>
<b>Figure 2.</b> The incidence of TB worldwide in 2014	<b>56</b>
<b>Figure 3.</b> Egypt Tuberculosis profile showing the incidence, prevalence and mortality rate of TB, MDR-TB and HIV patients with TB	<b>57</b>
<b>Figure 4.</b> The cell wall of MTB with the mycolic acids	<b>58</b>
<b>Figure 5.</b> The pathophysiology of MTB inside the host	<b>59</b>
<b>Figure 6.</b> The MTB bacilli after ZN staining under the microscope	<b>60</b>
<b>Figure 7.</b> Digital chest X-ray	<b>61</b>
<b>Figure 8.</b> Tuberculin assay	<b>62</b>
<b>Figure 9.</b> The Surface Plasmon Resonance of AuNPs	<b>63</b>
<b>Figure 10.</b> The FRET energy transfer	<b>64</b>
<b>Figure 11.</b> Geographic distribution of the samples collected in Egypt	<b>65</b>
<b>Figure 12.</b> Drug sensitivity results as obtained by culture	<b>66</b>
<b>Figure 13.</b> Gel electrophoresis of multiplex PCR	<b>67</b>
<b>Figure 14.</b> Amplification of randomly chosen samples by 16S-23S ITS primers	<b>68</b>
<b>Figure 15.</b> Sequencing peaks of sample 300	<b>69</b>
<b>Figure 16.</b> NCBI BLAST analysis of sample 300	<b>70</b>
<b>Figure 17.</b> Primers sites for amplification of expected mutation sites	<b>71</b>
<b>Figure 18.</b> Gel electrophoresis of MAS PCR	<b>72</b>
<b>Figure 19.</b> Anionic AuNPs characterization by SEM	<b>73</b>
<b>Figure 20.</b> Anionic AuNPs characterization by zeta sizer	<b>74</b>

<b>Figure 21.</b> SEM imaging of cationic AuNPs	<b>75</b>
<b>Figure 22.</b> Zeta sizer characterization of cationic AuNPs	<b>76</b>
<b>Figure 23.</b> Gel electrophoresis of <i>IS6110</i> amplification of bacterial strains	<b>77</b>
<b>Figure 24.</b> Gel electrophoresis of <i>rpoB</i> amplification of bacterial strains	<b>78</b>
<b>Figure 25.</b> Diagram of cationic AuNPs assay	<b>79</b>
<b>Figure 26.</b> Cationic AuNPs assay of <i>rpoB</i> amplicons of MTB DNA samples	<b>80</b>
<b>Figure 27.</b> Cationic AuNPs assay of <i>IS6110</i> amplicons of MTB DNA samples	<b>81</b>
<b>Figure 28.</b> Detection limit by Cationic AuNPs assay of <i>IS6110</i> amplicons	<b>82</b>
<b>Figure 29.</b> Diagram of FRET assay	<b>83</b>
<b>Figure 30.</b> FRET results by CY-3 16s rDNA specific probe	<b>84</b>

## LIST OF ABBREVIATIONS

<b>AuNPs:</b>	Gold Nanoparticles
<b>BCG:</b>	Bacillus Calmette-Guerin
<b>CY-3:</b>	Cyanine-3
<b>D:</b>	Aspartic acid
<b>dsDNA:</b>	Double Stranded DNA
<b>DST:</b>	Drug Susceptibility Testing
<b>FM:</b>	Fluorescent Microscopy
<b>FRET:</b>	Fluorescence Resonance Energy Transfer
<b>H:</b>	Histidine
<b>HIV:</b>	Human Immunodeficiency Virus
<b>ITS:</b>	Internal Transcribed Space
<b>LAM:</b>	Lipoarabinomannan
<b>LED:</b>	Light Emitting Diode
<b>LJ:</b>	Lowenstein-Jensen culture medium
<b>MAS:</b>	Multi Allele Specific
<b>MDR-TB:</b>	Multi-Drug Resistant Tuberculosis
<b>MODS:</b>	Microscopic Observation Drug Susceptibility
<b>MTB:</b>	<i>Mycobacterium tuberculosis</i>
<b>MTBC:</b>	<i>Mycobacterium tuberculosis</i> Complex
<b>NAATs:</b>	Nucleic Acid Amplification Techniques
<b>NFW:</b>	Nuclease Free Water
<b>NTM:</b>	Non-Tuberculous Mycobacterium

<b>P:</b>	Proline
<b>PCR:</b>	Polymerase Chain Reaction
<b>S:</b>	Serine
<b>SEM:</b>	Scanning Electron Microscopy
<b>SPR:</b>	Surface Plasmon Resonance
<b>ssDNA:</b>	Single Stranded DNA
<b>TB:</b>	Tuberculosis
<b>WHO:</b>	World Health Organization
<b>V:</b>	Valine
<b>VOC:</b>	Volatile Organic Compounds
<b>XDR-TB:</b>	Extreme Drug Resistant Tuberculosis
<b>Y:</b>	Tyrosine

## **Chapter 1: Introduction and literature review**

### **1.1. History of Tuberculosis (TB)**

Egyptian mummies 4000 years old revealed that TB was a common infection in ancient Egypt. It was also described by ancestor Assyrians and the Greeks. *Mycobacterium tuberculosis* (MTB) is believed to be a soil-living microorganism and developed to infect humans after serial mutations. It is postulated that the spread of TB to Europe was caused by the travelling of animals' merchants. Later in the modern history, TB killed quarter of Europe population in one of the most sever pandemics. Better medical precautions and then the introduction of the Bacillus Calmette-Guerin (BCG) vaccine sharply declined the morbidity and mortality rate [1]. Unfortunately, TB infection spread again due the development of drug resistance strains and the human immunodeficiency virus (HIV) pandemics especially in Africa where there are now high number patients co-infected with HIV and TB [1, 2].

### **1.2. Tuberculosis (TB)**

According to the 2014 World Health Organization (WHO) tuberculosis report, 1.5 million patients lost their lives to TB, of which one quarter were co-infected with HIV. This number exceeded the death rate of HIV alone which was 1.2 million people for the same year (**figure 1**). It is postulated that 9.6 million people carry MTB bacilli worldwide of which two thirds were infected in 2014 only (**figure 2**) [3]. According to the WHO reports about the incidence of TB in Egypt, half of the patients are still undiagnosed. In 2014, the incidence is 13 patients per 100,000 and the estimated number is 11,700 people with 1% MDR-TB and 6% of the patients are children (**figure 3**) [4]. TB is a contagious disease of the respiratory system and may progress to be extra pulmonary infection and disseminate to other organs such as the bones, lymph nodes, the brain, the spinal cord, the skin, the genital tract and the abdomen. It is important to note that not all carriers of MTB have the disease. According to the immune response of the host, some of them have active infection as the bacilli can

stay dormant for years. Malnutrition, poor aeration and low exposure to sun light and immune-comprising condition as co-infection with other disease like HIV are all essential factors that can activate the infection [1]. Therefore, TB is more prevalent in the developing countries where poverty prevails [5]. Limited resources affect accessibility to effective diagnostic methods and treatment. Also, poor medical awareness and poverty adversely affect compliance to treatment and thus increase incidence of drug resistance [6]. In efforts to control the global TB strike, WHO established the STOP TB program which has several missions in order to eradicate TB. It prepares road maps for adequate TB diagnosis, treatment and prevention. The organization main activities were divided into DOTS (Direct observed therapy, short courses) and research to innovate new drugs and vaccines. DOTS program served 32 million TB patients and contributed to the cure of 28 million people. Their services are also beneficial for MDR-TB and HIV patients [7]. The TB Research Movement that was developed by Stop TB Partnership and WHO, recommends the development of new diagnostic tools characterized by feasibility in limited resource settings, short turn-around time, cost-effectiveness, availability at the point of care (POC) level, possible differentiation between different TB forms (drug-sensitive, drug-resistant, or MDR-TB) and usefulness in pediatric TB patients [8].

### **1.3. *Mycobacterium tuberculosis***

The *Mycobacterium* genus is composed of *Mycobacterium tuberculosis* complex (MTBC) members, *M. Leprae* and non-tuberculous mycobacterium (NTM) [9]. MTBC has 8 members which are MTB, *M. canettii*, *M. africanum*, *M. bovis*, *M. caprae*, *M. microti*, *M. pinnipedii*, and *M. Bovis* and the attenuated BCG vaccine strain. However, only the MTB is the main causative agent of TB and the other species rarely cause human infection [10]. The name of genus is originated from term Myco- which means fungus due to their morphology which looks like fibers [11]. It is cultured on either solid medium as Lowenstein Jensen (LJ) and appears as clusters or on liquid culture medium (middlebrook 7H9 broth) where the growth is faster and appears as turbidity. Because the staining by carbol fuschin is not dissolved by acid-alcohol, it is called acid fast [12]. MTB bacilli are intracellular gram positive aerobic non-motile bacteria which infects macrophages [13]. The bacilli (0.5 to 3  $\mu$ m) are



well known by their long duplication time that reaches 20 hours [10,14]. The morphology of MTB bacilli may vary according to the surrounding media. For example, the MTB bacilli tend to be oval in shape in case of nutrient deficiency. Inside the macrophages, they look like fibers. Extreme drug resistant-TB (XDR-TB) may grow as branched filaments. The cell wall consists of two layers. The outer layer is composed of several proteins and lipids while the inner one is characterized by the presence of mycolic acids linked to peptidoglycan and arabinogalactan (**figure 4**). The peptidoglycan confers the bacilli its shape [15].

The genome of the reference strain MTB H37Ra consists of more than 4 million base pairs. It is characterized by the presence of about 200 out of 4000 genes for fat metabolism only which is considered relatively a high number. This explains the ability of MTB bacilli to use the host's cells as the carbon source. MTB does not have defined virulent factors. However, its ability to live inside the macrophages, production of certain proteins as katG and SodA which neutralize the toxic secretions of the macrophages and the rigid lipid rich cell wall (plays a key role in drug resistance) are the main defense mechanisms [1].

#### **1.4. Pathophysiology of TB**

Inhalation of only one to three bacilli is enough to induce infection. After inhalation of MTB bacilli most of the bacilli are exhaled away but some may sneak to the lower respiratory tract. The macrophages move to the site of infection and destroy the bacilli. In case of the failure of the macrophages to terminate the bacteria, the macrophages engulf the bacilli forming a tubercle where the bacteria remain dormant then solidifies and appears in chest x-ray. This is called Ghon complex and it is characterized by its low pH and oxygen deficiency. All these rigid conditions alter the bacilli replication but do not eradicate them. Moreover, they can stay dormant in these conditions for years [1, 12]. If the host's immunity becomes weaker, this granuloma may soften and the bacteria spread to the lung and other organs as the lymph nodes resulting in active infection [12]. The symptoms of the active disease are vague and non-specific. They include general fatigue, fever, night sweats and productive cough with or without hemorrhage, loss of appetite and therefore unexplained weight loss. That is why this disease is sometimes called "consumption" [11]. If the patient is left

untreated, MTB causes suffocation of the lungs by two scenarios: severe destruction of the lung tissues by decreasing the oxygen supply or granuloma softening which releases the bacilli. This process induces internal hemorrhage and tubercle formation which also suffocate the patient (**figure 5**) [1]. Although the rigid cell wall protects the bacilli, it is also one of the bacterial virulent factors. The cell wall components of the MTB are very distinctive due to the presence of glycolipid lipoarabinomannan (LAM) and lipopeptides [1, 11]. The mycolic acids allocated in a vertical position is the main bacilli protective shield. Phthiocerol dimycoerate is one of these acids which is referred by some authors as the wax ball surrounding the bacteria and its virulence is evidenced by its rareness in the attenuated strains [1]. In addition, the cell wall morphology is designed to inhibit the host's enzymatic degradation and neutralizes the destructive oxygen and nitrogen derivatives and in the same time, other cell wall components induce alveolar macrophages apoptosis. The phagocytosis of the MTB bacilli stimulates the secretion of inflammatory cytokines which induces bronchial inflammation and aids in granuloma development. Moreover, this process recruits the neutrophils, monocytes and lymphocytes, which accumulate in the site of infection and results in bronchoconstriction [11].

### **1.5. TB Vaccine**

In 1920, the BCG was invented from life attenuated *M. bovis* and is the only available vaccine. However, its efficiency is variant (0-80%) depending on the immune response of the vaccinated person. In USA, it is recommended for people at high risk only [12]. In Egypt, this vaccine is compulsory for all newborns.

### **1.6. TB treatment**

The treatment efficiency is affected by two factors; the bacilli may escape to shield themselves inside the macrophages so they become unreachable by the antibiotics. The second factor is the slow growth which alters the effect of the antibiotics because they are active against the bacteria during the growth. Also, drug resistance typically develops after prescribing regimens with a single antibiotic [10].

After reliance on streptomycin to treat TB, the British Medical Research council reported the first streptomycin resistant cases. It was concluded that multiple antibiotics should be administered to cure patients. Because rifampicin and isoniazid are the main drugs against TB, strains resistant to both antibiotics are described as MDR-TB. In the early 1990s, some countries as USA and Russia had reported high number of patients infected with resistant TB. Shortly, these reports were received from several other countries [6].

TB is defined as MDR-TB when it resists at least rifampicin and isoniazid [16, 17]. When the bacteria resist antibiotics from the first line and second line, it is called extreme drug resistant TB (XDR-TB) which will lead to patients' death due to lack of treatment [14].

The bacterial strain is called resistant when at least 1% of the bacterial population resists the antibiotic [18]. Primary resistance is when the patient is infected with a resistant strain and secondary which is more common, when the patient is infected with susceptible strain but due to inadequate treatment, the bacteria resist the drugs [14]. The anti-tuberculous drugs are divided into two categories; first line (**table 1**) and second line antibiotics.

### **1.6.1. First line antibiotics**

Rifampicin is an essential anti-tuberculous drug which inhibits the transcription of the  $\beta$ -subunit of the RNA polymerase. Most of rifampicin resistant strains have mutations in the 81-bp region of the *rpoB* gene which is called Rifampicin Resistance-Determining Region (RRDR) which are present in codons 507 to 533 [16, 17, 19]. The *rpoB* gene is the encoding gene of the  $\beta$ -subunit of RNA polymerase; a tetra subunit enzyme consists of  $\alpha$ ,  $\beta$ ,  $\beta'$  and  $\delta$  subunits. In addition, according to the mutation site, the resistance degree varies. Mutations in amino acid 526 and 531 result in high resistance while in 511, 516, 519 and 522 result in weaker resistance (MIC below 64  $\mu\text{g/ml}$ ). There is still probability of other mutations in the terminal amino acids and need for advanced tests in case of negative result of drug susceptibility test [15]. Isoniazid is the second main anti-tuberculous drug which is a prodrug activated in the human cell by bacterial catalase peroxidase. The bacteria resist this drug by

mutations in the enzyme encoding gene (*KatG*) to decrease its production. The mutations occur mainly in *KatG*, *inhA* genes and *inhA* promoter. Inside *KatG* only, there are several possible mutations and is responsible for 50-90% of isoniazid resistant cases. Mutations in other genes are proved to be responsible for isoniazid resistance as *KasA*, *aphC* and *ndh*. Resistance to isoniazid is most probably coupled with rifampicin resistance [15, 16]. Pyrazinamide is a prodrug used to treat TB activated by the enzyme pyrazinamidase in vivo [6, 15]. The bacteria resist it by about 120 different mutations in *pncA* gene. By molecular techniques, line probe was able to detect all these mutations accurately. However, testing the bacterial susceptibility by culture is not easy because the drug is active at acidic pH which inhibits the bacterial growth [15]. Ethambutol is activated in vivo and inhibits the attachment of the mycolic acids to the cell wall [6]. Resistance to it develops due to mutations in *embB* gene especially in codon 306 which represent 47-62% of the resistance cases. Other mutations in codons 330 and 630 result in ethambutol resistance as well. Streptomycin is an aminoglycoside antibiotic and is considered as second line in some references. Mutations in the genes *rrs* and *rpsL* are the common reason to develop resistance to streptomycin. However, other mutations in other genes can also cause resistance. Till now, there is no rapid method to test the susceptibility of tuberculosis to streptomycin [15]. Drug resistance mutation(s) are summarized in (table 2).

### **1.6.2. Second line antibiotics**

Fluoroquinolones, ethionamide and aminoglycosides as amikacin and kanamycin are all active antibiotics against TB [15]. The first line antibiotics are preferred because cure can be achieved after 6 months while when administering second line antibiotics, the treatment duration will extend to at least 18 months with less efficiency and more adverse effects [20].

### **1.7. TB diagnosis**

Early diagnosis of TB is necessary to eliminate inhalation transmission, prevent development of resistance and subsequently reduces death rate from this disease especially among HIV co-infected patients [21]. Despite the need for accurate

diagnosis of TB, sometimes presumptive diagnosis is done according to the patient's history and confirmed by smear microscopic testing and/or radiological findings [22, 23]. Also drug susceptibility testing (DST) is not performed until the treatment by the first line antibiotics fails or the patient has recurrent TB infection [24]. Timely TB diagnosis and drug susceptibility testing using culture-based methods are limited by the slow growth of the bacilli. Culturing the bacteria, determine whether it is typical or atypical and DST need weeks to perform. Moreover, positive results need rigid confirmation [6].

Further differential testing is now needed due to increase in NTM infections that cause similar clinical symptoms to that of MTB. NTMs were considered opportunistic infection until the breakthrough of HIV which increased incidence of NTM pulmonary infection [25, 26]. The essentiality of differentiation of Mycobacterium infections arises from the difference in the drugs regimens used to treat NTM [27]. All the diagnostic procedures are summarized in **table 3**.

WHO strongly recommends that the governments of the high burden countries should participate by a great impact to achieve the goals of END TB program. This program is launched by the WHO and has four main activities: early diagnosis of TB and DST in addition to regular screening of high risk people, treatment of patients carrying drug susceptible and resistant strains, co-operation with HIV programs and finally prevention of new infections and vaccines development [24].

### **1.7.1. Specimens collection and preservation**

Enough sputum should be expectorated by the patients. Some patients as the pediatrics and HIV patients have low sputum volume and/or low bacterial load in their sputum. Saline spray aids to increase the specimen volume but the patients need assistance to use it. The specimen collection and preservation importance arises when it is not analyzed on time or needs to travel for further investigation. The lung flute (Medical Acoustics, New York, USA), which is FDA approved, helps the patients to collect the sputum in-house. It is held by the patient's mouth and stimulates the lung to soften and expectorate the sputum. The second product is produced by Deton Corp. (Pasadena, USA) which is a big bag in which the patient coughs. It collects the

bacilli-containing droplets and the air is pulled out physically. After specimen collection, the second step is the preparation of the sample. OMNIgene SPUTUM (DNA Genotek Inc., Ottawa, Canada) produces a liquefaction, decontamination and preservation system for the samples without the need for freezing up to 8 days. The samples did not have any contamination when investigated on LJ media [24].

### **1.7.2. Microscopic observation**

The first line diagnostic method for MTB is smear microscopy which is 125 years old [12, 28]. It relies on staining of the acid fast bacilli using Ziehl Neelsen (ZN) stain (**figure 6**). It is fast and cheap so used heavily in poor-resources countries for TB diagnosis and monitoring the patients receiving anti-tuberculous antibiotics. With accuracy varying from 35% to 80%, additional diagnostic method must ascertain the negative sample because only one bacillus in the sample is enough to call the sample positive. However, 5,000 bacteria/ml are required to be present to allow bacilli detection by smear microscopy. Despite the great danger of TB spread from patients of high bacterial load, 17% of the misdiagnosed patients by smear microscopy due to their low bacterial load transmit the bacilli to their surrounding community [29]. So the false negative results are found among HIV patients and extra pulmonary TB patients. Also, it does not give information about the bacterial type, its activity and drug susceptibility [30]. It is useful to indicate active infection as only viable cell will retain the stain while the dead bacilli have leaking cell wall which won't retain the stain. Smear microscopy is recommended for the diagnosis of pulmonary TB with minimum of two sputum samples collected in two successive mornings. The sensitivity of smear microscopy can be enhanced by concentrating the sputum samples. However, this process needs sophisticated biosafety concerns for the working technician in addition to the long time consumed [3, 31]. The introduction of the fluorescence dyes to stain the MTB bacilli and the use of the fluorescent microscopy (FM) enhanced the sensitivity by 10%. Even sample preparation and examination extended for shorter time and allowed to increase the number of examined samples per day. The spread of the FM in peripheral laboratories was altered by the high cost of the bulb and the need for regular maintenance. The use of the potent light emitting diode (LED) allowed the spread of FM after replacing the bulb in peripheral laboratories due to its powerful light, lower cost, longer life time of

the bulb and elimination of the risk of exposure to mercury vapor in case of bulb breakage. WHO recommends the replacement of FM by LED microscopes for smear microscopy. The automated microscopy allowed the accurate screening of the fluorescent bacilli after manual preparation of the slides. They are accompanied by software that analyzes every field in the slide and needs only five minutes for complete slide analysis. This microscope dispensed the usage of Xpert MTB/RIF (NAAT diagnostic tool recommended by WHO and discussed alter) by 73% for TB diagnosis. Becton Dickinson Corp. (New Jersey, USA) also developed an automated system that stains the TB smears and analyzes them. its performance is nearly similar to LED-microscope [24]. WHO recommends the testing of the smear microscopy by the conventional or LED microscopy in the peripheral laboratories [29].

### **1.7.3. Digital chest X-ray**

Digital chest X-ray allows detection of MTB in resources limited settings recommended by the WHO. It is rapid and accurate even in HIV co-infected patients. Delft Imaging Systems (Veenendaal, Netherlands) developed the software CAD4TB to analyze the images to detect any lung abnormalities (**figure 7**) [24].

### **1.7.4. Biomarkers based MTB detection**

#### **1.7.4.1. Chromatographic detection of MTB**

Determine™ TB LAM Ag (Alere Inc., Waltham, Massachusetts, USA) is an immunochromatographic strip that detects the LAM which is a MTB glycolipid present in the living and disseminated bacilli. LAM is detected in the urine and is useful for the detection pulmonary and extra pulmonary TB and NTM. Recent studies reported that this assay is a useful indicator for severe infection in HIV patients [24, 29].

#### **1.7.4.2. Volatile organic compounds (VOC) for detection of MTB**

When TB infection is active, oxidative stress products, volatile compounds and nitric oxide are present in the patient's breath. The detection of these volatile compounds offers a non-invasive screening for TB patients [29]. TB Breathalyzer (Rapid

Biosensor Systems Ltd, UK) is an example device that detects these VOC by just coughing in a certain device and the result is available within 4 minutes.

### **1.7.5. Immuno-response based assays**

#### **1.7.5.1. Tuberculin test**

It is the injection of low concentration of TB antigen (protein purified derivative) subcutaneously. After 48 hours, the injection site becomes red due to immune reaction to the antigen (**figure 8**). The positive result in youth is most probably active infection. While in elderly, it may indicate latent infection or vaccination. After this test, chest x-ray, microscopic examination of sputum samples, culture and molecular diagnosis should be performed. The main drawback is the inability of the test to differentiate the active from latent infection and from BCG vaccine [12, 29].

#### **1.7.5.2. Serological assays**

These assays detect MTB indirectly through capturing the anti-tuberculous antibodies. ELISA and LAM-ELISA detect LAM. However, The WHO recommendation is to avoid using the blood but use the urine to diagnose TB either pulmonary or extra-pulmonary. The assay also can't differentiate between the viable and dead bacilli. The sensitivity for pulmonary and extra-pulmonary TB was 65% and 55% respectively. Serological test costs about \$30 per sample and there is high possibility of false negative results [32]. Because the commercial serological tests detect the antibodies, they do not differentiate between recent and old infection or even between infection and vaccination [29]. TB Interferon-Gamma Release Assays (IGRAs) are other example of serological tests that detect the  $\gamma$ -interferon released by the white blood cells of the infected people. Due to its poor sensitivity, it does not distinguish between active and latent infection. WHO recommends it only in poor resource countries [33].

#### **1.7.6. Bacterial culture**

According to the WHO protocol, smear microscopy and culture are done from sputum collected in the early morning from 3 consecutive days. Decontamination of the



sputum is a primary step. It is always done by the traditional NAOH-N-acetyl cysteine based method. A recent kit called Decomics (Salubris Inc., Massachusetts, USA) utilizes beads of high absorption capacity and specific chemicals for proper decontamination of sputum [29]. Culture is the second step in the diagnosis and it is considered the gold standard method for both MTB detection and DST. Several solid culture media are used for isolation, identification, species differentiation and DST as Lowenstein-Jensen (LJ), middlebrook 7H10 and blood agar. However, due to the slow metabolic activity of MTB, species identification and DST require several weeks to obtain conclusive results which extend to 2 and 6 weeks for liquid and solid culture medium, respectively [29]. The sensitivity of the culture is 100 bacteria/ml. The culture doesn't allow differentiation of MTB from NTM by initial culture because the colonies morphology is nearly identical [29, 34, 35]. The essentiality of species differentiation comes from the presence of inherently resistance for specific antibiotics. For example; *M. bovis*, BCG, and *M. canettii* have innate resistant to pyrazinamide [36, 37]. Molecular assays, biochemical tests or additional culture for 2 to 4 weeks are recommended for species discrimination [38, 39]. For example, LJ medium containing glycerol is used to allow the growth of MTB and inhibits the growth of *M. bovis*. When isolation of *M. bovis* is required, pyruvate is added to the culture medium instead of glycerol [40, 41]. Several improvements have been introduced to benefit from the sensitivity of the culture and overcome the drawback which is the long duration. Microscopic observation drug susceptibility (MODS) involves the microscopic examination of the liquid culture media (middlebrook 7H9) by inverted light microscope and the duration of the test is 9 days. MODS is used for MTB differentiation from NTM by the addition of para-benzoic acid which inhibits the growth of MTB only. The incorporation of antibiotics to the culture media was exploited to perform DST by MODS [29, 42]. Also the growth patterns differ according to the species so differentiation was allowed by MODS [43]. Culture-based DST is performed by several assays as nitrate reductase and colorimetric redox indicator (CRI). All these methods are based on culturing bacteria on drug-containing culture media. The color change indicates the ability of the resistant bacteria to grow in the presence of the antibiotic of interest and to perform certain reaction indicating the presence of resistant strains. Although the accuracy of these methods reaches 99%, the long time to obtain the results which extends to 2 weeks limits their application [44-48].

Another type of the liquid culture is the automated liquid culture. A famous example is Bactec 960 MGIT (Beckton Dickson) which is enriched by oleic acid, albumin, dextrose and catalase to enhance the MTB bacilli growth. Drugs as polymyxin B, amphotericin B, nalidixic acid and trimethoprim are added to prevent contamination. The growth of MTB bacilli is hastened to about 7 to 10 days and the growth is detected by either colorimetric or fluorometric detection. Species differentiation and DST can also be performed. However, this method needs expensive instruments and trained personnel. In addition, the problem of radioactive waste products is an issue [3, 29]. WHO recommends performing the culture including the MODS, CRI and nitrate reductase in the reference laboratories only [29].

#### **1.7.7. Nucleic Acids Amplification Techniques (NAATs)**

For tuberculosis to be detected by molecular test, the bacteria should disseminate to the blood stream, urine, sputum and the affected organs. Molecular assays allow detection of MTB in clinical samples, differentiation of MTB from NTM, DST and performing epidemiological studies. The results are reproducible when the sample is smear positive and accuracy reaches more than 95%. It saves the costs of isolation of patients suspected to have be infected with MDR-TB or XDR-TB and cost saving is up to \$15,000 per year [49, 50]. However, in some cases as extra pulmonary TB, culture is needed before performing the NAATs to increase the amount of the DNA [27].

Polymerase chain reaction (PCR) and isothermal amplification are the most common approaches of amplification of nucleic acid. Although the performance time extends to 8 hours, NAATs are much faster than culture. So these tests are the most beneficial in life threatening cases as meningitis MTB where smear microscopy is not suitable and the culture time can be too long to save the patient's life [29]. Despite the development of many molecular techniques as commercial kits and in-house assays, LPAs (Hain Lifescience, Nehren, Germany); INNO-LipA (Fuji-Rebio Europe, Göteborg, Sweden); and Xpert® MTB/RIF (Cepheid, California, USA) are the only WHO approved molecular assays to detect MTB [24]. WHO recommends the molecular tests for smear positive samples when the patients had not administered any antibiotics (the first sample or the first smear positive sample are the suitable samples). The sensitivity is 95% and the specificity is up to 100%. However, they are

recommended when the sample is smear and culture positive. While the sensitivity drops dramatically when the smear is negative and the culture is positive for the following reasons. The number of the bacteria is very few and the DNA extraction is faced by the strong cell wall of the bacteria. A recent study evaluated Amplicor-MTB (Roche, Risch-Rotkreuz, Switzerland), BD Probe (Becton Dickson) and transcription mediated amplification; the sensitivity was about 97% although the specificity varied from 71% to 96% for smear positive/culture positive samples. However, for smear negative/culture positive samples, the sensitivity ranged from 57% to 76%. Moreover, factors as the type of the sample and storage, the DNA extraction and amplification protocol, the visualization method of the hybridization and the presence of any inhibitors or contaminants will affect the accuracy [10]. So these tests are useful to confirm infection rapidly. Also, these assays require complex infrastructure for DNA extraction and test performing. The personnel should also be well-trained and work according to standard procedures. The risk of contamination can be overcome by the use of automated systems. However, the cost will be high due to the regular maintenance and the required reagents. Despite the presence of several assays, the lack of standardization limits their approval by the FDA. So till now, the gold standard methods for TB diagnosis are the smear microscopy confirmed by culture, and selective culture for DST. The diagnosis of TB patients co-infected with HIV, pediatric TB patients and extra pulmonary TB by sputum samples needs further investigation [29]. Despite the great sensitivity of molecular assays, the culture is still the most sensitive diagnostic tool. Most NAATs tests can't detect TB in blood samples. They can't be used to monitor the effectiveness of the therapy as the bacteria will be detected whether alive or dead [51]. One study revealed positive PCR results from patients successfully cured 2 years ago [52].

Sequencing of the 16s rDNA and 16S-23S internal transcribes spacer (ITS) is considered one of the most accurate detection methods for MTB [9, 25, 53]. The sequence of this region varies from 270 to 360 bp according to the species and thus amplification of this region followed by sequencing allows species differentiation [54]. The sequence of interest is compared to libraries as Genbank, the Ribosomal Differentiation of medical Microsystems databases and European molecular biology laboratory [9]. Comparison between commercially available NAATs for MTB detection is presented in **table 4**. The pipeline of NAATs for TB diagnosis is illustrated in **table 5**.

The variable region 16s rDNA is one of the most common sequences to target [55]. The gene 16s rDNA has 1500 bp. However, the first 500 bp are conserved among all MTB strains. So sequencing allows the exploration of unknown species [9]. Also *IS6110* which is a non-coding insertion sequence is used frequently for direct detection of MTB due its repetition up to 25 times in the whole genome and was detected by several primers from sputum samples [22, 56]. Specific targets within *rpoB* gene are widely applied to allow detection of MTB DNA and differentiate it from other mycobacterium. According to the primers, the *rpoB* gene is used either to detect MTB or to detect mutations responsible for rifampicin resistance [16, 18]. Targets within other genes as gene of 32, 38 or 65 KD protein, *recA* , *hsp65*, *dnaJ*, *sodA* and 16S-23S rRNA, , *groE1*, or *mtb-4* genes are also used to detect MTB [9, 29]. WHO recommendations about NAATs are in **table 6**.

#### **1.7.7.1. Automated MTB detection assays**

COBAS® TaqMan® MTB (Roche Diagnostics) investigates 44 samples in the same time by the real time PCR. Liquefaction, decontamination and concentration of the sputum or bronchial lavage sample are a must before performing the assay. It detects the 16S RNA by real time PCR and the data is interpreted and stored automatically. The sensitivity is 96.4% for smear and culture positive specimens and drops to 76.8% for smear negative/culture positive. The detection limit is 18 bacilli/ml. Molecular Realtime MTB (Abbott, Chicago, IL, USA) is another assay that detects MTB DNA from NAOH-N-acetyl-L-cysteine treated sputum or bronchial lavage specimens. DNA extraction can also be automated. The operation time to extract and analyze 94 samples (its capacity) extends for 7 hours. The detection limit is 17 bacilli. The sensitivity is 97% for smear and culture positive and 81% when the smear is negative. Due to the cost of the device, its wide usage is limited in the resource-limited countries. An automated assay that detects MTB DNA by molecular beacons is Fluorotype® MTB (Hain Lifescience). The DNA is amplified with the molecular beacons and the fluorescence is detected by specific software. Smear/ culture positive and smear negative/culture positive are diagnosed by sensitivity 100% and 90% respectively. This assay is also developed to detect MDR-TB. BD MAX™ platform (Becton Dickinson) which is still under development, utilizes real time PCR to detect MTB and to identify MDR. Its performance capacity is 24 samples in each run [24].

#### **1.7.7.2. Autonomous MTB detection assays**

These assays are not automated so they require the usage of several devices, complicated infrastructure and trained personnel. The Anyplex (Bio-Rad Laboratories, Hercules, California, USA) utilizes multiplex PCR to detect MTB, investigate MDR-TB and XDR-TB. The primers are designed by specific software and sample preparation should be performed before using this assay. The second example is MeltPro® Drug-Resistant TB Testing Kits (Xiamen Zeesan Biotech Co. Ltd, Hong Kong, China) that detects point mutation of rifampicin and isoniazid by real time PCR. Further development are done to achieve the detection of ethambutol, streptomycin and fluoroquinolones resistance [24].

#### **1.7.7.3. Line probe assays**

GenoType® MTBDRplus (Hain Lifescience) and INNO-LipA Rif.TB (Fuji-Rebio Europe) were the first assays approved by WHO for MTB and MDR-TB detection. They also allow species differentiation from NTM and investigate resistance to first line and second line antibiotics. Their costs are affordable for the high burden countries. The samples should be DNA extracted from culture and amplified to attach biotin and immobilized on nitrocellulose. The probes are attached to streptavidin-bound enzyme that allows colorimetric interpretation of the results which are then analyzed by certain software [24].

#### **1.7.7.4. DNA microarrays**

DNA microarrays depend on determining sequences within the 16s rRNA by fluorescence-labeled probes. The intensity of the fluorescence is proportional to the hybridization pattern and is measured by fluorescent microscopy. The results are available within few hours [10]. They are considered simplified form of line probe assays. The Autogenomics INFINITI® PLUS Analyzer platform (AutoGenomics, Vista, USA) is approved by FDA and can test 48 samples in 3.5 hours. The MTB Identification Array Kit (CapitalBio, Beijing, China) is used for MTB detection and

differentiation. The *M. Tuberculosis* Drug Resistance Detection Array Kit (CapitalBio) is used for MTB detection and identification of rifampicin and isoniazid resistance. TruArray® MDR-TB (Akonni Biosystems, Frederick, USA) is another microarray test that detects MTB and differentiates it from *M. avium* by using multiplex PCR to amplify the DNA and the fluorescence is detected by TRUdiagnosis software. VereMTB™ Detection Kit (Veredus Laboratories, Singapore) contains 500 probes by which it identifies the MTB through targeting the *IS6110* and 16S RNA, allows species differentiation from 8 NTM species and identifies rifampicin and isoniazid associated mutations [24].

#### **1.7.7.5. Modular, cartridge-based, fully automated NAAT**

Xpert® MTB/RIF (Cepheid Inc.) is the only NAATs diagnostic assay approved by WHO for MTB detection [24]. Performing the test takes about 2 hours with only one step done manually and the reagent can be kept at room temperature for one and half year. The assay detects MTB and rifampicin resistance accurately especially when the sample is smear and culture positive [24, 29]. It has modules for sample preparation and semi-nested PCR of *rpoB* for investigation of rifampicin resistance. WHO recommends its use for the diagnosis of suspected MDR-TB, HIV patients and for TB meningitis diagnosis [24].

#### **1.7.7.6. Semi-automated NAATs**

Eiken's Loopamp™ (Eiken Chemical Co. Ltd, Japan) MTB kit detects MTB from sputum samples without any pretreatment in the lysis tube by loop mediated amplification. Heating is used for MTB bacilli lysis [24]. It is an isothermal amplification assay which depends of amplification only of the target sequences when present. The hybridization action is investigated by gel electrophoresis to ensure the formation of the DNA target size. Also the double strand binds to SYBR green dye and the solution becomes green. However, when the target sequence is absent, the color of the solution remains orange. In both case, screening by ultraviolet is done [29].

### **1.7.8. Detection of TB by phage-display**

The concept of these detection approaches is the use of a specific phage that infects only viable MTB bacilli. The number of phages is proportional to the number of bacterial cells. The sensitivity and specificity for smear positive are 87% and 88% and for smear negative/culture positive are 67% and 98%. The test needs 2-3 days to get results and is considered a cheap diagnostic method. The available test in the market is FASTPlaque TB assay (Biotic laboratories Ltd., Ipswich, UK). Another assay is Phage amplified biological assays (Pha B) which utilizes the mycobacteriophage D<sub>29</sub> detects the bacteria in only 24 hours. However, the sensitivity is only 31%. The Phage Tek MB assay (Organon Teknika, Durham, NC, USA) is also available in the market but its low sensitivity limits its use. Another assay utilizes a phage that translates the luciferase enzyme. When the phage infects the bacteria, it oxidizes luciferin using ATP. Light is generated indicating the presence of viable mycobacteria so this assay can also be used to test the susceptibility of the bacteria. The light intensity is measured by a luminometer and results are generated within 2 days [9, 29].

### **1.7.9. Detection of TB by nanoparticles**

#### **1.7.9.1. Gold nanoparticles (AuNPs)**

Spherical AuNPs has average size from 0.8 to 250 nm. The large volume: surface area ratio is responsible for the activity of AuNPs where the bulk gold lacks this property. AuNPs are widely used due to their Surface Plasmon resonance (SPR) which results from the collective oscillation of the electrons of the conduction band (**figure 9**). This gives the solution its red color and the absorption peak is at 520 nm for 20 nm AuNPs. The solution of the AuNPs turns blue upon their aggregations which red shifts the absorption to 620 nm due to plasmon coupling of the aggregated AuNPs. This sensitivity is widely exploited to detect biological molecules as antigens, antibodies and DNA sequences [28, 57]. In addition, AuNPs are biocompatible so they are suitable for biological application. They can be manipulated to display several properties based on their particle size, surface charge, shape and inter-particle spaces [53]. The diversity of the AuNPs size and morphology allowed their use as scaffolds for the development of innovative assays platforms. The introduction of the AuNPs as fluorophore's quencher was investigated 40 years ago. Fluorescence resonance energy

transfer (FRET) technology is defined as spectroscopic approach to measure distances in the range of 30-80 Å [58, 59]. AuNPs can absorb excitation energy from several dyes in the same time [60]. The donor particle (dye or the fluorophore) is excited by a certain wave length and this excitation energy is transferred to the acceptor (AuNPs) (**figure 10**). This non-radiative energy is dependent on the space between the donor and the acceptor [58, 60, 61]. The rate of the energy transfer is inversely proportional to the sixth power space between the fluorophore and the quencher [62]. Recently, the application of AuNPs as fluorescence quencher is useful for disease diagnosis by capturing a specific DNA sequence by its complementary probe. Because the hybridization energy is 80 kcal/mol and extremely exceed the adsorption energy of the fluorophore on the AuNPs surfaces (8-16 kcal/mol), the DNA probes favors the hybridization with their complementary targets [58, 62]. Absorption was found to be the prominent behavior of 40 nm AuNPs. Larger particles were found to enhance the fluorescence by scattering [59]. The factors affecting the non-radiative energy transfer between the AuNPs and the fluorophores are the morphology and the diameter of the AuNPs, the distance spacing the AuNPs from the fluorophore and the intersection of the emission of the fluorophore and the absorption of the AuNPs [63]. Several diseases were accurately diagnosed by FRET technology by detection of the DNA such as herpes simplex, Gilbert's syndrome, parasites as malaria and toxoplasmosis, fungal infection as invasive aspergillosis and candidiasis [64-66].

#### **1.7.9.1.1. AuNPs synthesis**

AuNPs synthesis is attempted by either top-down or bottom up pathway. The first pathway means the synthesis of AuNPs from bulk particles. The second pathway which is more common allows the AuNPs to grow from the corresponding chemicals and the size is controlled [67]. The gold salt is dissolved in a suitable solvent and reduced to its ground valence state by a reducing agent as the citrate which also stabilizes the AuNPs by prohibiting their aggregation. By controlling the reaction parameters which are the reducing agent type and concentration, time and temperature, the desired morphology and size of the AuNPs is achieved. The simple citrate reduction method was introduced 65 years ago [68]. The synthesis is performed by reducing the gold derivative (gold (III) chloride trihydrate) to Au<sup>0</sup> by sodium citrate dibasic trihydrate. The citrate can be replaced by another reducing



agent according to the AuNPs of interest [68, 69]. When thiolated AuNPs are desired to be synthesized, the Shiffrin method is followed [68]. The affinity between the gold and thiol is exploited to stabilize the gold by an alkylthiol as DDT (dodecanethiol) and the reduction is performed by sodium borohydride dissolved in toluene. The thiolated AuNPs can be functionalized through antigen-antibody or streptavidin-biotin linkage with thiol groups. These particles are manipulated to allow detection of antigens, DNA specific sequences, peptides or carbohydrates [67-70].

#### **1.7.9.1.2. Modified AuNPs for MTB detection**

Thiol groups attached to the oligonucleotides and hence allow the binding of the AuNPs. If the target is present in the sample, the complementary sequences will anneal and AuNPs become free and aggregate in the presence of NaCl. The aggregation induces a color change from red to blue due to the SPR of the AuNPs. Soo *et al.*, developed AuNPs based assay to detect MTB by targeting *IS6110* and Rv3618 with amplicons of nested PCR and double probes specific for each target. The probes were linked to thiolated AuNPs and hybridization with complementary DNA sequence in the positive samples induced the visible color change from red to violet due to the shortening of the inter-particle space of the AuNPs. MTB and MTBC were detected with 96.6% sensitivity and 98.9% specificity, and 94.7% sensitivity and 99.6% specificity, respectively [71]. Baptista *et al.*, detected MTB DNA from clinical samples targeting the *rpoB* region. The detection limit was 0.75 µg [72]. Costa *et al.* developed another AuNPs based assay to detect MTBC and differentiation of MTB from *M. bovis*. Specific probes targeting the gene *gyrB* were allowed to hybridize with the amplified DNA [73]. Liandris *et al.* targeted 16S-23S ITS using AuNPs modified probes specific for MTB. Unamplified DNA was detected with a detection limit of 18.75 ng [74]. Das *et al.*, developed AuNPs based biosensor by depositing zirconium oxide linked to MTB specific probe on gold surface. The probe was linked to the zirconium by exploiting the affinity between the oxygen atom of the phosphate backbone of ssDNA and zirconium atoms. The detection limit of the biosensor was 0.065 ng/µl. [75].

### 1.7.9.1.3. Unmodified AuNPs for MTB detection

Thiolated AuNPs synthesis needs long time and is relatively cumbersome [26]. So the use of unmodified AuNPs saves the time, effort and cost of surface biofunctionalization. Hussain *et al.* detected MTB using 16s rDNA specific oligotargeter. Amplified and genomic MTB DNA were detected successfully and the sensitivity was 100% compared to genus and species specific semi-nested PCR [55]. Tsai *et al.*, used unmodified AuNPs to detect amplified DNA by targeting *IS6110*. In case of positive samples, the probe hybridized with its target and the resulting charge of dsDNA was negative. The repulsion between the dsDNA and the negatively charged AuNPs resulted in AuNPs aggregation the color was changed from red to blue. If the target DNA is absent, the DNA probes would remain attracted to the AuNPs and prevent their aggregation and consequently, the color of the solution remained red. The detection limit for this assay is 2.6 nM [26]. The characteristics of the previous assays are compared in **table 7**.

### 1.7.9.2. Detection of TB by FRET

FRET-based detection of TB and drug resistance mutations were investigated by several research groups. Hwang *et al.* used upconversion nanoparticles (UNNPs) made of rare earth lanthanide elements. The assay depends on biotinylated PCR amplification of the *IS6110* sequence of MTBC, mixing with the UCNPs conjugated with streptavidin (FRET donor) and addition of SYTOX orange dye that is intercalated in dsDNA (FRET acceptor). The decrease in green fluorescence of the UCNPs reports the presence and hybridization of the biotinylated PCR amplicon (*IS6110*) to the streptavidin activated UCNPs [76]. Another research group designed an assay that involves sandwich-form FRET for detection of the MTBC using cadmium telluride quantum dots (donor) and AuNPs (acceptor) that are both coupled to different oligonucleotides. The target region is the early secretory antigen target-6 (ESAT-6) DNA which is conserved among all the MTBC members and is not present in *M. bovis* so allows differentiation of infection from vaccination [77]. Isoniazid resistance has been also investigated by FRET. Saribas *et al.* used real-time PCR and labeled probes to detect single nucleotide point mutations in the genes *inhA*, *KatG* and *ahpC* because they are known to involve the mutations responsible for isoniazid resistance. Two labeled probes were used: one is short probe (sensor) that hybridizes

at the site of mutation of interest and the longer probe (anchor) hybridizes next to it. When both probes become in close proximity, high fluorescence is observed. Gradual increase in the temperature is applied until the sensor probe is not attached anymore and a massive drop in the fluorescence is observed. The temperature at which the probe is detached is called the melting temperature. Discrimination between INH-susceptible from resistant strains is allowed because the resistant strains have a different melting temperature different than the wild strains [78]. El-Haji et al. detected all the rifampicin associated mutations in the *rpoB* gene in a single assay using wave length shifting molecular beacons. The MTB DNA was extracted from sputum samples, detected by amplifying 16s rDNA region for species differentiation then the 81-bp region within the *rpoB* gene was amplified with specific primers. The amplicons are allowed to anneal with five beacons linked to five different fluorophores. Each molecular beacon is complementary for a certain mutation site. In case of the presence of any mutation, the molecular beacon won't be able to hybridize and the fluorescence will not appear. Subsequently, only the wild type MTB will emit the five fluorescence colors. The molecular beacons were modified to be wave length shifting to allow the emission of longer wave length and better discrimination among the five fluorophores [79]. Qin *et al*, detected the MTB bacilli through fluorescent silica nanoparticles and SYBR- green attached to anti-tuberculous antibodies. The specific antibodies attach to the bacilli and the double emission of the two dyes indicates the presence of MTB bacilli [62]. Ekrami *et al*, used mouse monoclonal antibodies linked to silica fluorescent nanoparticles for direct detection of MTB bacilli from sputum samples. The anti-tuberculous antibodies are attracted to the surface antigens of the MTB and intense fluorescence was observed [80]. The FRET based assays are illustrated in **table 8**.

## **1.8. Thesis scope and objectives**

- 1.8.1.** Development of colorimetric nano-sensor for detection of MTB DNA using cationic AuNPs.
  
- 1.8.2.** Development of AuNPs-based FRET sensor for the fluorometric detection of MTB DNA.

## Chapter 2: Materials and Methods

### 2.1. Clinical bacterial strains

This study was performed after getting IRB approval from the American University in Cairo case #2014-2015-149 and the approval of the Egyptian Ministry of Health No. 2-2015/1. Seventy two anonymous mycobacterial samples from the Central Laboratories archive were used in this study (**figures 11, 12**). The geographic distribution was 24 patients from Abassia Chest Hospital, Cairo governorate, 15 patients from Giza Chest Hospital, Giza governorate, 13 patients from Alexandria Governorate, 11 patients from Dakahlia Governorate, 2 patients from Suez Governorate, 2 patients from Helwan City, 1 patient from Matarai City, 1 patient from Isamlia Governorate, 1 patient from Elmenya Governorate and 1 patient from the Central Laboratories of Ministry of Health.

All the samples were cultured on LJ liquid medium according to the manufacturer's protocol. The culture is done from early morning sputum samples of the Egyptian patients from different regions all over Egypt. The patients were diagnosed to be infected with Mycobacterium. None of the samples were known to be whether typical or atypical Mycobacterium. Reference bacterial strains include *M. tuberculosis* H37Ra (positive reference strain) and *Mycobacterium smegmatis* (negative reference strains). Four *E.coli* samples, *Acinetobacter baumannii* ATCC 17978, *Pseudomonas aeruginosa* ATCC 27853, *Klebsiella pneumonia* ATCC 23495 and *Enterobacter aerogenes* ATCC 13048 were the negative samples.

### 2.2. DNA extraction

Extraction was performed using QIAamp DNA mini extraction kit (Cat no. 51304, Qiagen, Hilden, Germany). According to the extraction protocol of gram positive bacteria, cell wall lysis is required prior to extraction. It is accomplished by adding the bacterial pellet to lysozyme enzyme 20 µg/ml (from chicken egg white, cat no. 41800, Norgen Biotek Corp., Thorold, Canada) dissolved in 20 mM Tris- Hcl, PH 8 (cat. no. 10812846001, Sigma Aldrich, Missouri, USA), 2 mM EDTA (cat. no. 431788, Sigma

Aldrich) and 1.2 % triton (cat. no. x100, Sigma Aldrich) and incubated for 30 min at 37 °C. Then the extraction protocol for gram positive protocol is followed according to the manufacturer's protocol. Extraction of the DNA from the gram negative was done according to the manufacturer's protocol.

### **2.3. Identification of the bacterial strains by PCR**

#### **2.3.1. Species differentiation using Multiplex PCR**

Identification of the samples (n=72) to differentiate MTB from NTM was achieved by multiplex PCR. Two sets of primers targeting the *rpoB* region were used [30]. All the primers are manufactured by BioBasic, Markham, Canada. The primers and the amplicons size are illustrated in **table 9**. The reaction mixture volume was 20 µl and prepared by mixing 10 µl master mix (cat. no. RR310A, Takara Bio. Inc., Shiga, Japan), 0.75 µl of each primer type from stock concentration 10 µM, 2 µl of DNA samples and 5 µl of nuclease free water (NFW). The reaction conditions are denaturation for 3 min at 95 °C and 1 min at 97 °C, 2 cycles for 1 min at 95°C, 30 sec at 64 °C and 1 min at 72 °C, 2 cycles for 1 min 95 °C, 30 sec at 62 °C and 1 min at 72 °C, 2 cycles for 1 mi at 95°C, 30 sec at 60 °C, 1 min at 72 °C, 2 cycles for 1 min at 95 °C, 30 sec at 60 °C and 1 mi at 72 °C, 2 cycles for 1 min at 95 °C, 30 sec at 58 °C and 1 min at 72 °C, 22 cycles for 1 min at 95 °C, 30 sec at 56 °C and 1 min at 72 °C and 1 cycle at 72 °C for 10 min [30]. The PCR reaction was done using the thermal cycler (Veriti, Applied Biosystems CA, USA). All the amplicons were examined on 1.5% w/v agarose gel electrophoresis stained with ethidium bromide.

#### **2.3.2. Amplification of 16S-23S ITS and Sequencing**

Thirteen samples were chosen randomly to be sequenced. Primers for amplification the region 16S-23S ITS region were chosen from literature. The primers sequences are: MYITSF (5'-GATTGGGACGAAGTCGTAACAAG-3') and MYITSR (5'-AGCCTCCCACGTCCTTCATCGGCT-3'), manufactured by BioBasic. The reaction mixture volume was 50 µl and prepared by mixing 25 µl master mix (cat. no. RR310A, Takara Bio. Inc.), 1.875 µl of both the forward and reverse primer type from stock solution 10 µM , 5 µl of DNA template and 12.5 µl of NFW. The amplification conditions were slightly modified to initial denaturation at 95 °C for 5 min followed

by 35 cycles of (95 °C for 1 min, 55 °C for 30 sec and 72 °C for 1 min) , and 72 °C for 7 min (1 cycle) [30]. Thirteen samples (92, 272, 187, 392, 300, 445, 348, 100, 98, 265, 447, 394, and 114) were chosen randomly and amplified (**table 10**). All the amplicons were examined on 2% agarose for gel electrophoresis and then were sequenced by MacroGen (Seoul, South Korea). Then the forward and reverse sequences were assembled by AlignX Vector NTI 11.5 software (Life technologies, Carlsbad, California, USA) and finally analyzed by NCBI database.

### **2.3.3. Identification of drug resistance mutations of MDR-TB by Multiplex Allele Specific (MAS) PCR**

The reaction mixture was 25 µl prepared as follows: 12.5 µl master mix (cat. no. RR310A, Takara), 1 pmol rpoB 516, 5 pmol rpoB526 , 32.5 pmol rpoB531 , 30 pmol RIRm , 1 pmol katG0F, 1 pmol katG5R , 2 µl of DNA template and the final volume is completed by NFW (**tables 11, 12**). The PCR conditions consisted of an initial denaturation at 96 °C for 3 min, 25 cycles of 95°C for 50 sec, 68°C for 40 sec, and 72°C for 60 sec, and a final extension at 72°C for 7 min [81]. Amplicons were visualized on 2% wt/vol agarose gel stained with ethidium bromide.

## **2.4. AuNPs-based sensors for MTB DNA detection**

### **2.4.1. Cationic AuNPs-based sensor**

#### **2.4.1.1. Cationic AuNPs synthesis**

Ten milliliter of 0.1% (w/v) chitosan (cat. no. 448869 Sigma Aldrich) in 1% acetic acid was allowed to boil, then 0.5 ml of preheated 10mM gold (III) chloride trihydrate (cat. no. 520918, Sigma Aldrich) added and mixed for 45 min. Characterization was performed by Zeta sizer (Malvern Zeta sizer 3000HSA; Malvern Instruments Ltd., Malvern, UK) and Scanning electron microscope (SEM) (LEO SUPRA 55; Carl Zeiss AG, Oberkochen, Germany).

#### **2.4.1.2. Amplification of MTB DNA by *IS6110* primers**

PCR was performed with 5µl (50 ng) of template DNA in a reaction mixture (50 µl) containing 12.5 µl master mix (cat. no. RR310A, Takara), 1 µM primer from each

forward 5'-CCTGCGAGCGTAGGCGTCGG-3' and reverse 5'-CTCGTCCAGCGCCGCTTCGG-3'. The PCR started with a denaturation step (94°C for 3 min), followed by 35 cycles of denaturation (94°C for 1 min), annealing (68°C for 1 min), and extension (72°C for 1 min), and a final extension step at 72°C for 5 min as described by Kocagoz et al. [21]. Amplicons were visualized on 1.5% wt/vol agarose gel stained with ethidium bromide.

#### **2.4.1.3. Amplification of MTB DNA by *rpoB* primers**

PCR was performed with 5µl (50 ng) of template DNA in a reaction mixture (50 µl) 12.5 µl master mix (cat. no. RR310A, Takara), 1 µM primer (each) (forward 5'-CGTACGGTCGGCGAGCTGATCCAA -3' and reverse 5'-CCACCAGTCGGCGCTTGTGGGTCAA -3'). The PCR conditions are 95 °C for 5 min, 30 cycles at 95°C for 30 sec, then at 72°C for 60 sec, and 72°C for 5 min as described before [26]. Amplicons were visualized on 1.5% wt/vol agarose gel stained with ethidium bromide.

#### **2.4.1.4. Cationic AuNPs assay**

The assay was performed by mixing 5µl of the cationic AuNPs and 20ul of amplified product. The mixture left for 10 minutes before detection the color change.

#### **2.4.1.5. Detection limit for cationic AuNPs assay**

Serial dilutions were prepared after amplifying MTB H37Ra sample. The initial DNA concentration was calculated by measuring the absorption at 260 and 280 nm using UV-Vis spectrophotometer (model 7315, Jenway, UK). DNA concentration was calculated using the following equation:

$$\text{DNA Concentration } (\mu\text{g/ml}) = (A_{260} \text{ reading} - A_{320} \text{ reading}) \times \text{dilution factor} \times 50 \mu\text{g/ml}$$



## **2.4.2. AuNPs-based FRET sensor for detection of MTB**

### **2.4.2.1. Anionic AuNPs synthesis**

Citrate reduction method of AuNPs was followed as previously described [68]. Briefly, 35 ml of 0.25 mM gold (III) chloride trihydrate (cat. no. 520918, Sigma Aldrich) and equal volume of 2.5 mM of sodium citrate dibasic trihydrate (cat. no. C7254, Sigma Aldrich) were placed separately in two glass beakers, covered with aluminum foil and heated. When the gold (III) chloride trihydrate started to boil, sodium citrate was added and left to stir for 40 minutes till the solution color turned bright red. For concentration, 1.5 ml of the colloid solution was centrifuged at 14,000 rpm for 20 minutes, and then the supernatant was dissolved in 200  $\mu$ l nuclease free water. Characterization was performed by zeta sizer and SEM.

### **2.4.2.2. Probe sequence**

CY-3 labeled 16s rDNA specific probe was used. The sequence of the probe was CY-3- 5' CACCACAAGACATGCATCCCG-3' (BioBasic) [55].

### **2.4.2.3. Optimization of the FRET assay**

Hybridization buffer was prepared as follows; 2.5  $\mu$ l of 500 mM NaCl, 1  $\mu$ l of 1 $\mu$ M CY-3 labeled probe and the final volume is completed to 10  $\mu$ l by NFW. Serial dilutions of the AuNPs were added to the hybridization buffer. Fluorescence was measured to detect the optimum concentration of AuNPs for the assay; excitation and emission were measured at 544 and 584 nm [82], respectively (BMG Labtech 413-3179, Ortenberg, Germany).

### **2.4.2.4. Detection of MTB DNA using FRET assay**

Extracted DNA was added to 8 $\mu$ l hybridization buffer then fragmented by 5% sonication at 50 °C for 10 min dark (Sonorex digital 10p, Bandelin, Dusseldorf, Germany). Then the samples were subjected to denaturation for 3 min at 95 °C

followed by annealing at 52 °C for 45 sec by the thermal cycler. After incubation at room temperature for 15 min, 40 µL of AuNPs were added to each sample. Excitation and emission were measured at 544 and 584 nm, respectively.

#### **2.4.2.5. Detection limit of FRET assay**

Serial dilutions of H37Ra reference strain sample were prepared and the test was run as previously described. The initial DNA concentration was calculated by measuring the absorption at 260 and 280 nm using UV-Vis spectrophotometer. DNA concentration was calculated using the following equation:

$$\text{DNA Concentration } (\mu\text{g/ml}) = (A_{260} \text{ reading} - A_{320} \text{ reading}) \times \text{dilution factor} \times 50 \mu\text{g/ml}$$

#### **2.5. Data interpretation and statistical analysis:**

The sensitivity and specificity were calculated by the following equations:

$$\text{Sensitivity} = \text{no. of true positive} / (\text{no. of true positive} + \text{no. of false negative}) \times 100$$

$$\text{Specificity} = \text{no. of true negative} / (\text{no. of true negative} + \text{no. of false positive}) \times 100$$

Relative fluorescence was calculated for each test by normalizing fluorescence values against residual fluorescence values. Unpaired Mann-Whitney U test was used for comparison between the two sample sets (GraphPad Prism version 4.0 for Windows, San Diego California, USA).

## Chapter 3: Results

### 3.1. Clinical bacterial strains

Mycobacterial DNA was extracted from 72 clinical isolates of infected patients. Patients' gender distribution was 57 males and 15 females. All 72 Mycobacterial samples were characterized by multiplex PCR and FRET. Two reference strains of *M. smegmatis* and H37Ra were cultivated and used as negative and positive controls, respectively. Isolates of different non-mycobacterial pathogens were also recruited and investigated by both multiplex PCR and FRET. They involved four *E.coli* strains, *Acinetobacter baumannii*, *Pseudomonas aeruginosa*, *Klebsiella pneumonia* and *Enterobacter aerogenes*.

### 3.2. Characterization of the bacterial strains by PCR

#### 3.2.1. Species differentiation by Multiplex PCR

DNA extracted from all (n=72) isolates (mycobacterial and non-mycobacterial) was amplified via multiplex PCR, and then analyzed by gel electrophoresis. Based on amplicon size reported by primer-BLAST of utilized primers, a clear 235 bp band was observed for H37Ra sample (positive control), while *M. smegmatis* (negative control) yielded band at 136 bp. Accordingly, 70/72 of tested samples yielded bands at 235 bp and were classified as MTB, while 2/72 yielded bands at 136 bp and were classified as NTM (**figure 13**). All amplicons of non-mycobacterial pathogens yielded no bands on gel electrophoresis.

#### 3.2.2. Amplification of 16S-23S ITS and Sequencing

Randomly selected 13 samples out of total 72 samples (13/72) had amplicon size of 350 bp on gel electrophoresis (**figure 14**). Such samples were subjected to forward and reverse sequencing. Clear sharp peaks with limited background noise appeared in the sequencing results (**figures 15, 16**). The forward and reverse sequences were assembled and analyzed by NCBI database. Twelve samples (12/13) were reported as MTB while only one sample (1/13) was reported as NTM (*M. kansasii*). The concordance of the sequencing with the FRET assay was 100%.

### **3.2.3. Identification of drug resistance mutation of MDR-TB by MAS- PCR**

According to the results of DST conducted on cultures, 8 samples were found to be rifampicin resistant, 12 samples were isoniazid resistant and 5 samples were MDR-TB. The remaining samples were susceptible to rifampicin and isoniazid. Two NTM samples were reported among the isoniazid resistant samples. The samples were investigated by MAS PCR in which one of the primers is attached at a certain site and the other primers are supposed to attach in the mutation site in case of wild type only (**figure 17**). Concerning rifampicin resistance, 4 from 8 resistance mutations were identified: two samples had mutation in the position *rpoB* 516; other two had mutation at *rpoB* 531. For isoniazid resistance, only 3 samples from 12 were found to have the mutation in *KatG* 315. None of drug susceptible samples had any mutations when investigated by PCR (**figure 18**).

### **3.3. AuNPs based sensors for MTB DNA detection**

#### **3.3.1. AuNPs Characterization**

Characterization of anionic and cationic AuNPs was performed by SEM and Zeta sizer. SEM images showed spherical particles of uniform size and shape (**figures 19, 21**). The average diameters of anionic and cationic AuNPs were 40 nm and 20 nm, respectively. Zeta sizer report revealed similar sizes' distribution and zeta potential of -19 mV for the anionic AuNPs (**figures 20, 22**).

#### **3.3.2. Cationic AuNPs-based sensor**

##### **3.3.2.1. IS6110 amplification of MTB DNA**

All the 72 samples were amplified by the *IS6110*-specific primers according to previously discussed conditions. Amplicons were tested on the gel electrophoresis. All MTB samples have band at 123 bp (**figure 23**). None of the negative strains had bands on gel.

### **3.3.2.2. *rpoB* amplification of MTB DNA**

All the 72 samples were amplified by the *rpoB*-specific primers according to previously discussed conditions. Amplicons were tested on the gel electrophoresis. All MTB samples had band at 235 bp (**figure 24**). None of the negative strains had bands on gel electrophoresis.

### **3.3.2.3. Cationic AuNPs assay and Detection Limit**

The presence of amplified DNA products provided a color shift of the cationic AuNPs from red to blue (**figure 25**). Amplified MTB clinical samples showed violet-to-blue color with AuNPs. The red color of AuNPs persisted after adding PCR products of negative controls (**figures 26, 27**). Serial dilutions of the MTB H37Ra were prepared and investigated by the cationic AuNPs assay. By calculating the initial DNA concentration, the detection limit was found to be 5.4 ng/ $\mu$ l (**figure 28**).

### **3.3.3. AuNPs-based FRET assay for MTB DNA detection**

#### **3.3.3.1. Optimization of FRET assay and investigation of the clinical bacterial strains by FRET**

The least volume of the AuNPs to induce complete quenching of the fluorescence was determined by mixing gradual volumes of the AuNPs and the hybridization buffer containing CY-3 probe. The least volume that induced complete quenching was 40  $\mu$ l (**table 13**).

For proof-of-concept (**figure 29**), we first tested samples of both positive (MTB H37Ra) and negative (*M. smegmatis*) controls by multiplex PCR and FRET assay. Both assays succeeded to discriminate between samples. By FRET assay, the fluorescence yield of positive control exceeded 3-fold higher than that of negative control.

FRET assay was performed on all 72 samples of mycobacterial species. Seventy samples (70/72) were identified to be MTB by multiplex PCR, of which, sixty nine samples displayed fluorescence 3-fold higher than the negative control, so exceeding the proposed cut off value. Only 1 sample had lower fluorescence than the cut off value, which means a false negative result. Two samples (2/72) were identified to be

NTM by multiplex PCR and FRET, both displayed fluorescence 3-fold lower than that of the negative control, indicating that they were NTM.

Also, 8 negative samples which are the non-mycobacterial pathogens (four *E. coli* samples, *Acinetobacter baumannii*, *Pseudomonas aeruginosa*, *Klebsiella pneumonia*, and *Enterobacter aerogenes*) were investigated by both multiplex PCR and FRET. Only the *Enterobacter aerogenes* sample had a high fluorescence exceeding the cut off value which means it is a false positive result. The remaining seven samples had lower fluorescence than the cut off value.

To summarize, of total 72 Mycobacterium samples tested, one false negative was recorded; of 8 non-mycobacterial samples, one false positive was detected, translating to sensitivity and specificity of 98.6% and 90%, respectively. The concordance between the Multiplex PCR and FRET methods was 98% (**figure 30**).

#### **3.3.3.2. Detection limit by FRET**

Serial dilutions of the sample H37Ra were prepared to detect the detection limit of the FRET assay. The initial DNA concentration was found to be 40 ng/ $\mu$ l, and the detection limit is 10 ng/ $\mu$ l. So the detection limit for the assay without prior DNA amplification was determined to be 10 ng/ $\mu$ l (**table 14**).

## Chapter 4. Discussion

TB diagnosis has always been challenging, since accuracy, affordability and short time-to-result are critical properties of a novel assay for point-of-care. Two AuNPs-based MTB assays developed in this study offer rapid and accurate method for MTB detection utilizing the minimum laboratory infrastructure. The main purpose of the two assays is differentiation of MTB from NTM as initial culture does not allow species differentiation because the colonies morphology of most mycobacteria species is nearly the same. So differential culture, biochemical assays or molecular assays are required for species differentiation [10].

Seventy two anonymous sputum samples were collected from patients from different regions in Egypt. The sputum was decontaminated and cultured on LJ media in the Central laboratories. MTB H37Ra and *M. smegmatis* were the positive and negative control and were also cultured on LJ media in addition to 8 negative strains. The DNA was extracted according to the manufacturer's protocol. DNA extraction of the mycobacterial species and other gram positive species was started by lysis of the rigid cell wall by lysozyme enzyme.

Characterization of the clinical samples was verified by multiplex PCR to allow the differentiation of MTB form NTM. Two sets of primers were used and each of them amplifies its target and yields amplicons of different sizes. The primers are specific for the region *rpoB* region which allowed species differentiation due to its variability to differentiate between mycobacterial species. The MTB samples yielded amplicons of size 235 bp while NTM samples yielded amplicons at 136 bp when they were analyzed by gel electrophoresis. Seventy samples were characterized as MTB and only two samples were found to be NTM.

Further verification of the samples was done by sequencing. Random samples were chosen and amplified by 16S-23S ITS specific primers. All the amplicons were 350 bp in size. This hindered differentiation of MTB from NTM sample because the amplicons size is nearly the same but the sequence is different. The amplicons were then subjected to forward and reverse primer walking sequencing followed by

assembling by AlignX Vector NTI 11.5 software. Then finally the resulting sequences from the assembly were analyzed by NCBI database. The sequencing result was 12 MTB samples and 1 sample was NTM (*M. kansasii*). The concordance between the sequencing and the multiplex PCR was 100%.

MAS-PCR was used to report the most common point mutations associated with MDR-TB, since rifampicin and isoniazid are the most powerful antibiotics against MTB bacilli. DST was first performed by culture in the Central laboratories. MAS-PCR was done using 4 sets of primers to identify the point mutations. In case of wild type, the selected primers properly hybridized to the DNA template and amplify it. In case of mutation in the hybridization site, primers could not hybridize to the target and no amplicons were obtained. This reaction was highly specific and sensitive to detect single point mutation. The reported DST profiles were compared with PCR results. Only the main mutations were detected within the *rpoB* for rifampicin resistance and *KatG* for isoniazid resistance. Concerning rifampicin resistance, 4 from 8 resistance mutations were identified: two samples had mutation in the position *rpoB* 516; other two had mutation in the *rpoB* 531. For isoniazid resistance, only 3 samples from 12 were found to have the mutation in *KatG* 315. The resistant samples of undetected mutation have other mutations which are less common and were not investigated by their corresponding primers here.

Two AuNPs-based sensors were developed to allow colorimetric and fluorometric detection of MTB. The first sensor is the AuNPs-based sensor for colorimetric detection of MTB DNA. The targets were *IS6110* and *rpoB* genes. *IS6110* is a non-encoding insertion transposal sequence and repeated up to 25 times along the MTB genome. It has been a common target when developing assay targeting MTB [22, 56]. The *rpoB* gene is encoding for the  $\beta$ -subunit of RNA-polymerase of MTB and has been targeted by distinctive primers for either MTB detection or identification of rifampicin resistance associated mutations [16, 18]. The cationic AuNPs were synthesized using chitosan, acetic acid and gold (III) chloride trihydrate. The AuNPs were spherical in shape with average diameter 20 nm. The principle of the cationic AuNPs assay is based on the unique physicochemical properties known as SPR, which is responsible for characteristic color of the AuNPs. Freely dispersed AuNPs show a red color. When the inter-particle distance decreases, the color changes from



red to blue due to the red shift in the absorption spectrum to a higher wave length in the UV-visible spectrum. The change in the absorption results from the plasmon-plasmon coupling of the aggregated AuNPs [69]. In case of positive samples where the target DNA sequence is present, the amplicons are yielded after hybridization of the primers. Negative-charged DNA were attracted to positively- charged AuNPs, leading to their aggregation, thus, color shifts from red to blue. However, in case of negative samples, no amplicons were obtained and AuNPs remained dispersed, thanks to the repulsion forces between the AuNPs which keep the intra-particle distances constant. Subsequently, the color remains red and no color shift occurs. The detection limit was determined by preparing serial dilutions of MTB H37Ra samples. Initial DNA concentration was calculated after measuring the samples absorption at 260 and 280 nm and was found to be 40 ng/ $\mu$ l. The last tube that displayed color change contained 5.4 ng/ $\mu$ l DNA (detection limit).

The second sensor was AuNPs-based FRET for fluorometric detection of unamplified MTB DNA. Citrate reduction method was attempted for the synthesis of anionic AuNPs. Sodium citrate dibasic trihydrate was used to reduce the gold (III) chloride trihydrate. The result was citrate coated AuNPs of negative charge. The AuNPs size was 40 nm because this size displays the maximum absorption capacity so offers sufficient quenching of the fluorescence. The CY-3 dye was chosen because it has been used extensively to evaluate FRET phenomenon. The excitation and emission (544 and 584 nm) were measured according to the previous experiments [59, 61, 63]. The probe sequence was chosen to target 16s rDNA region because it has hyper variable regions that differentiate the different species of the mycobacterium genus and has been investigated before to allow accurate detection of MTB by AuNPs [9, 55]. The assay was first optimized by setting the minimum AuNPs volume sufficient to induce the maximum fluorescence quenching. This was accessed by gradually increasing volumes of AuNPs added to the hybridization buffer using blank sample (water) instead of DNA. The adequate volume was found to be 40  $\mu$ l of 40 nm AuNPs while larger volumes did not decrease the fluorescence significantly. The anonymous samples (n=72) in addition to the positive and negative controls were investigated by FRET sensor. When the target MTB DNA was present, the probe hybridized with the CY-3-16s rDNA specific probe and the more stable dsDNA structure was formed.

This exposes the negatively charged phosphate backbone to the outer media where the negatively charged AuNPs are present; resulting in repulsion and adsorption of the AuNPs to the DNA is prevented. Consequently, the AuNPs is spaced from CY-3 and fluorescence is emitted. In case of absence of the target DNA as in the *M. smegmatis* and the negative controls, the AuNPs become in close proximity to the CY-3 probe and quench the fluorescence for the following reasons. First, there is binding affinity of CY-3 fluorophore towards AuNPs (the energy of the hybridization is 80-100 kcal/mol and the adsorption energy of the fluorophore on the AuNPs surface is 8-16 kcal/mol ) [59]. Second, the inter-particle repulsion between the AuNPs enhances the adsorption of the AuNPs on the CY-3 labeled probe. Third, the non-radiative energy transfer between the AuNPs and the CY-3 (fluorophore) enhances the quenching of the fluorescence [83]. By FRET, 69 from 72 samples were found to be MTB which means they had relative fluorescence exceeding the estimated cut-off value that was three folds the negative control. Of total 72 Mycobacterium samples tested, one false negative was recorded; of 8 non-mycobacterial samples, one false positive was detected, translating to sensitivity and specificity of 98.6% and 90%, respectively. The concordance between the multiplex PCR and FRET methods was 98%. The concordance of the FRET assay, multiplex PCR, and sequencing was 100%.

The detection limit was determined by the DNA of the reference strain MTB H37Ra. Serial dilutions were prepared of the sample then the hybridization buffer was prepared. The least concentration that displayed fluorescence higher than the relative cut-off value was the detection limit. The initial sample concentration was calculated after measuring the absorption at 260 and 280 nm and was found to be 40 ng/ $\mu$ l. The last positive fluorescence was obtained after the dilution of the sample to the quarter so the detection limit of the assay 10 ng/ $\mu$ l.

## **Chapter 5: Conclusion and Future Perspectives**

Fast and accurate diagnosis leads to better clinical and socioeconomic outcomes. Also reduces the chances for the spread of the disease will be precluded and the development of drug resistance will be averted. So the drug regimens will be shorter and more effective.

The developed assays detected MTB DNA with high accuracy and sensitivity. The cationic AuNPs based assay detected the amplicons of the MTB DNA by just one step which is the addition of the AuNPs. The color change is observed visually without the need for any instruments. This assay can circumvent the gel electrophoresis that needs several preparation steps and the use of the toxic chemical ethidium bromide. The second assay is the AuNPs-based FRET assay. The DNA was not exposed to previous enzymatic digestion and amplification. The preparation of the sample needs simple steps after the DNA extraction. The assay is performed by just the use of the CY-3 probe and the cost of the amplification is saved. The results are obtained shortly after the DNA is extracted by observing the fluorescence. The cut-off value was the 3 times of the base fluorescence and the positive samples are obviously discriminated from the negative samples. Due to the low cost and accuracy of the FRET assay, it can be extended for the diagnosis of TB in limited resources countries.

Several developments can be introduced to improve the detection of TB. Non-sputum samples as the saliva, urine and the exhaled air should be validated for culturing and further investigation. DNA extraction may be improved by the use of beads to replace the sophisticated and expensive extraction kits. The colorimetric assay performance can be improved by the development of specific reader to avoid personal difference when judging color change and the results are analyzed spectrophotometrically. Also drug resistance can be investigated by the use of specific probes for the mutation sites. The FRET assay can be easily manipulated to detect the resistance associated mutations. Probes specific for the mutation points can be synthesized tagged to specific fluorophore. Different fluorophores with distinctive excitation and emission can be used to allow the diagnosis and DST in the same time.

## 6- Tables

**Table 1. First line antibiotics, mode of action and main adverse effects [2, 6, 16, 84, 85]**

<b>Drug name</b>	<b>Characteristics</b>	<b>Mode of action</b>	<b>Main adverse effects</b>
Rifampicin	Semisynthetic derivative of rifamycin	Inhibits the transcription of the $\beta$ -subunit of the RNA polymerase	- Allergic reaction - Gastrointestinal discomfort
Isoniazid	Prodrug which is activated in the human cell by bacterial catalase peroxidase	Alters the synthesis of the mycolic acids	- Neuropathy - Allergic reaction in the skin
Ethambutol	Activated in vivo	Inhibits the attachment of the mycolic acids to the cell wall	- Reversible optic neuritis
Streptomycin	Aminoglycoside antibiotic	Inhibits bacterial proteins synthesis by binding to the 30S ribosomes subunit which is involved in translation of mRNA	- Renal toxicity - Ototoxicity
Pyrazinamide	Prodrug used to treat tuberculosis activated by the enzyme pyrazinamidase	Increases the pH of the cytoplasm so alters the normal membrane pressure	- Gastrointestinal discomfort - Allergic reaction - Liver toxicity

**Table 2. Genes of the common mutation(s) in the resistant MTB strains [2, 6, 16, 17, 84-87]**

Drug	Genes of common mutation(s) in resistant strains	Normal gene role	Frequency relative to the resistant strains	Mutation site	Effect of the associated mutation
Rifampicin	<i>RpoB</i> 81-bp region which is called Rifampicin Resistance-Determining Region (RRDR)	$\beta$ -subunit of RNA polymerase	90-95%	526( H to P, D, Y)	High resistance
				531 (S to L)	High resistance
				511( L to P)	Low resistance
				516 (D to V , Y)	High resistance
				519 (N to Y)	Low resistance
Isoniazid	<i>InhA</i>	Production of enoyl-acyl carrier protein reductase	30%	522 (S to L)	Low resistance
	<i>inhA</i> promoter		30%	15	Moderate resistance
	<i>KatG</i>	Production of catalase and peroxidase	50-90%	315 (S to L)	Moderate resistance
Pyrizamide	<i>PncA</i>	Production of the activating enzyme: pyrazinamidase	60%	120 different point mutations	High resistance
Ethambutol	<i>embB</i>	Arabinosyl transferase	20-70%	306	Moderate resistance
				330	High resistance
				630	High resistance
Streptomycin	<i>RpsL</i>	The ribosomal protein S12 production	52-59%	330	High resistance
				630	High resistance

**Table 3. Comparison between the most applicable diagnostic approaches of TB.**

<b>Diagnostic approach</b>	<b>Target</b>	<b>Advantage</b>	<b>Disadvantage</b>	<b>References</b>
Smear microscopy	MTB bacilli	- Fast, cheap, simple	-Low sensitivity up to 50% -Misdiagnose HIV co-infected patients due to their low bacterial load	[29, 30]
Tuberculin skin test	TB proteins	-Fast, cheap, simple -Can detect latent infection	-Does not discriminate between infection and vaccination so yields false positive results -Additional assays should be done to confirm infection	[12, 29, 30]
Culture	MTB bacilli	-Accurate and sensitive -Allows drug susceptibility testing	-Need long time to obtain the results - Costly infrastructure - The personnel need prior training for safety - Does not allow species differentiation	[29]
Serological assays	Anti-tuberculous antibodies	-Does not need complicated infrastructure -Discriminate infection from vaccination	- Sensitivity is low in HIV patients	[29, 32]
NAATs	DNA	- Fast and accurate - Allows species differentiation - Allows DST - Low contamination risk	-Costly infrastructure and consumables -Trained personnel are required	[10, 29, 38, 51]

**Table 4. Commercially available NAATs for MTB detection**

Reaction type	Assay's name and fabricator	Target	Specimen type	Sensitivity	Ref.
Real time PCR	Cobas Amplicor, Roche	16s rDNA	Clinical specimens	93%	[10, 29, 38, 88-93]
Nested real time PCR	GeneXpert MTB/Rif , Cepheid	<i>rpoB</i> gene	Clinical specimens	90%	[29, 94-96]
Isothermal transcription mediated amplification	Amplified Mycobacterium tuberculosis direct, Genprobe	rRNA	Clinical specimens	93%	[10, 29, 52, 97, 98]
Strand displacement amplification	Becton Dickson, BD probe tech	<i>IS6110</i> and 16srDNA	Clinical specimens	93%	[10, 29, 38, 90, 99, 100]
Loop mediate amplification	LAMP , Eiken, Japan	16s rRNA, <i>gyrB</i>	Sputum samples	_____	[29, 93, 101]
Polymerase chain reaction	Inno-LiPA Rif.TB line probe assay , Innogenetics, Belgium	16s-23s rRNA	Sputum and culture samples	100%	[29, 38, 90]
Polymerase chain reaction	Genotype Mycobacterium and Genotype MTBDR plus assay, Hain lifescience, Germany	23s rRNA, Mutations in <i>rpoB</i> , <i>KatG</i> and <i>inhA</i> genes	Sputum and culture samples	90%	[29, 38, 90]

**Table 5. Pipeline for the development phases of TB diagnostic technologies.**  
Retrieved from [24].

**A. High complexity assays.**

Early development	Late or completed development	On pathway to WHO evaluation
<b>Molecular- Detection/DST</b>		
<p>New TruArray MDR-TB (Akkoni) COBAS TaqMan MTB + DST (Roche) Hydra 1K (Insilixa) Mycobacterium Real-time MDR (CapitalBio) Aries (Luminex) PNAclap (Panagene) AccuPower TB&amp;MDR (Bioneer)</p>	<p>TRC Rapid MTB (Tosoh) VereMTB (Veredus laboratories) LiPA Pyrazinamide (Nipro) Fluorotype MTBDR (Hain) TBMDx (Abbott) Meltpro (Zeesan) Mycobacteria RT PCR (CapitalBio) REBA MTB-XDR (YD Diagnostics) EasyNAT TB (Ustar) BD Max (BD)</p>	<p>GenoTYPE MTBDRsi (Hain) LiPA MDR-TB (Nipro) REBA MTB-Rifa (YD Diagnostics)</p>
<b>Culture-based – Detection/DST</b>		
<p>BNP Middlebrook (NanoLogix) Rapid colorimetric DST</p>	<p>TREK Sensitive MYCOTB (Trek)</p>	



## B. Moderate complexity assays.

Early development	Late or completed development	On pathway to WHO evaluation
<b>Molecular Detection/DST</b>		
Xtend XDR (Cepheid) Alere Q (Alere) Enigra ML (Enigra Diagnostics) Q-POC (QuantuMDx) EOSCAPE (Wave80) TBDx system (KGI) X1 (Xagenic) MTB Detection (Tangen Biosciences)	Genedrive MTB/RIF (Epistem) Truelab/Truenat MTB (Molbio) Xpert Ultra (Cepheid)	TB LAMP (Eiken)
<b>Cellular Response- Detection/Latent and Latent to active progression</b>		
T-Track TB (Lophius) TAM-TB (LMU/Alere) EAST-6/CFP-10 skin test (SSI)		QuantiFERON-TB PLUS (Qiagen) Diaskin (Generium)
<b>Breath biomarker-Detection</b>		
BreathLink (Menssana) Prototype breathalyzer (Next Dimensions Tech) TB Breathalyser (Rapid Biosensor Systems) Aeonose (The eNose Company)		

**C. Low complexity assays.**



<b>Antigen, Antibody and Biomarker detection- Detection</b>		
LAM in sputum (Standard Diagnostics)		Alere Determine TB-LAM in urine (Alere)
IRISA-TB (Antrum Biotec)		
<b>Enzymatic-Detection/DST</b>		
$\beta$ -lactamase reporter (Global BioDiagnostics)		

**Table 6. WHO recommendation: Role of NAATs in TB diagnosis. Retrieved from [24].**

Test	Location	Throughput	Function	Test complexity	Hardware cost	Cost/test
WGS	Ref.	High	Surveillance/ DST/ treatment	High	High	High
Genotyping	Ref.	High/ moderate	Surveillance	High	High	High/ moderate
Automated batched PCR	Ref.	High/ Moderate	MTB Dx	High	High	Low
High-income country NAATS	Ref./Int.	High/ moderate	MTB/NTM Dx	High	High	Moderate
Microarrays	Ref./Int.	Moderate	MTB/NTM Dx DST <sup>a</sup>	High	High	High/ moderate
LPA	Ref./Int.	Moderate	MTB/NTM/ Dx/ DST <sup>a,b</sup>	Moderate	Moderate	Moderate
Modular NAATs	Ref./Int.	Moderate	Dx/DST <sup>b</sup>	Low	High	Moderate
SSM replacement	Int./Per.	Moderate/ Low	Dx/DST <sup>b</sup>	Low	Moderate/ low	Low

a: assays can be used in NTM

b: DST can be used also for TB diagnosis

Dx: Diagnosis

DST: Drug Susceptibility Testing

WGS: Whole Genome Sequencing

Ref.: Reference laboratory, Int.: Intermediate Laboratory, Per.: Peripheral Laboratory

**Table 7. Comparison between the main diagnostic assays for detection of MTB by AuNPs.**

<b>AuNPs type</b>	<b>Size of spherical AuNPs</b>	<b>Sample</b>	<b>PCR cycles</b>	<b>Turnaround time</b>	<b>Target</b>	<b>Sensitivity and specificity</b>	<b>Detection limit</b>	<b>Ref.</b>
un modified AuNPs	14 nm	DNA extracted from culture, digested by BamH1 enzyme	16s rDNA : 30 cycle, Semi-nested PCR: 25 cycles	1 hour	16s rDNA	100% and 100%	1 ng/μl for PCR product/ 40 ng for genomic DNA	[55]
	13 nm	Blood samples	35 cycles	1 hour	<i>IS6110</i>	—	2.6 nM	[28]

Thiolated AuNPs	13 nm	Cultures	35 cycles	25-40 min	gyrB locus	—	—	[73]
	—	49 sputum, 6 bronchial washes, 7 pleural effusion, 6 urine and 5 blood samples.	30 cycles	—	RNA polymerase $\beta$ _subunit	100%	0.75 $\mu\text{g}/\mu\text{l}$	[72]
	15-20 nm	Stool samples			16S-23S ITS DNA	87.5% and 100%	18.75 ng/ $\mu\text{l}$	[74]
	13.7 nm	DNA extracted from cultures prepared from sputum samples	40 cycles and 14 cycles	1 day	<i>IS6110</i> , Rv 3618 DNA	96.6% and 98.9% for MTBC and 94.7% and 99.6% for MTB	0.5 pmol	[71]

**Table 8. Assays developed for fluorometric detection of MTB**

<b>Assay type</b>	<b>Fluorophore</b>	<b>Target</b>	<b>Sensitivity and specificity</b>	<b>Ref.</b>
Upconversion nanoparticles detection of MTBC	Lanthanide nanoparticles and SYTOX orange dye	<i>IS6110</i>	100% and 100%	[76]
Sandwich-form AuNPs based FRET for detection of the MTBC	Cadmium telluride quantum dots	ESAT-6	94.2% and 86.6%	[77]
Drug resistance detection by Real-time PCR	LCRed640 and fluorescein	Point mutations in the genes <i>inhA</i> , <i>KatG</i> and <i>ahpC</i>	76% and 100%	[78]
Drug resistance detection by molecular beacons	Texas red, fluorescein, tetrachlorofluorescein, tetramethylrhodamine, rhodamine	<i>rpoB</i> gene	97% and 100%	[79]
Detection of MTB bacilli	Fluorescent silica nanoparticles and SYBR-green	MTB bacilli	—	[62]
Detection of MTB bacilli	Monoclonal antibodies with fluorescent silica nanoparticles	MTB bacilli	97.1% and 91.35%	[80]

**Table 9. The primers and amplicons sizes used to differentiate between MTB and NTM**

Forward primer	Reverse primer	Amplicon size in bp	Identification	Ref.
5'- TACGGTCGGCGAGCT GATCCAAA-3'	5'- ACAGTCGGCGCTTG TGGGTCAAC-3'	235	MTB	[30]
5'- GGAGCGGATGACCAC CCAGGACGTC-3'	5'- CAGCGGGTTGTTCT GGTCCATGAAC-3'	136	NTB	[30]

MTB: *Mycobacterium tuberculosis*

NTM: Non-tuberculous Mycobacterium

**Table 10. Samples chosen randomly and their sequencing results**

<b>Sequenced Samples</b>	<b>Sequencing result</b>	<b>Reference</b>
95	NTM	Alexandria governorate
272	MTB	Abasia chest hospital, Cairo governorate
187	MTB	Dakahlia governorate
392	MTB	Giza chest hospital, Giza governorate
300	MTB	Dakahlia governorate
445	MTB	Abasia chest hospital, Cairo governorate
348	MTB	Alexandria governorate
100	MTB	Alexandria governorate
98	MTB	Alexandria governorate
265	MTB	Abasia chest hospital, Cairo governorate
447	MTB	Abasia chest hospital, Cairo governorate
394	MTB	Giza chest hospital, Cairo governorate
114	MTB	Alexandria governorate




**Table 11. The primers used for identification of drug resistance associated mutations [80]**

Target site of mutation	Primer	Forward primer	Primer	Reverse primer	Amplicon size
KatG at 315	KatG5R	5'-ATACGACCTCGATGCCGCT-3'	KatG0F	5'-GCAGATGGGGCTGATCTACG-3'	293
rpoB at 516	rpoB516	5'-CAGCTGAGCCAATTCATGGAC-3'	RIFm	5'-TTGACCCGCGCGTACAC-3'	218
rpoB at 526	rpoB526	5'-CTGTCGGGGTTGACCCA-3'	RIFm	5'-TTGACCCGCGCGTACAC-3'	185
rpoB at 531	rpoB531	5'-CACAAAGCGCCGACTGTC-3'	RIFm	5'-TTGACCCGCGCGTACAC-3'	170

**Table 12. Amplicons size by MAS PCR. The presence of specific band size indicates wild type while the absence of specific band size indicated mutation and drug resistance.**


Mutation site	Amplicon size in bp
KatG 315	293
rpoB 516	218
rpoB 526	185
rpoB 531	170

**Table 13. Optimization of AuNPs concentration for optimum quenching of fluorescence.** The red arrow is pointed at the optimum AuNPs volume used in the FRET assay to quench the fluorescence.

40 nm AuNPs dilutions	Fluorescence
Hybridization buffer (10 $\mu$ l) + 40 $\mu$ l NFW	59185
Hybridization buffer + 30 $\mu$ l NFW +10 $\mu$ l AuNPs	21908
Hybridization buffer + 20 $\mu$ l NFW +20 $\mu$ l AuNPs	12782
Hybridization buffer + 10 $\mu$ l NFW +30 $\mu$ l AuNPs	1235
 Hybridization buffer + 40 $\mu$ l AuNPs	968
Hybridization buffer + 50 $\mu$ l AuNPs	955

**Table 14. Detection limit of FRET assay investigated by H37Ra sample.**

Serial dilution of the DNA were prepared and fragmented in the hybridization buffer then investigated by the FRET assay. The red arrow is pointed at the least DNA concentration detected by FRET.

Positive control	Relative fluorescence
H37Ra	33.5
 H37Ra (1/4)	14.4
H37Ra (1/16)	1.228
H37Ra (1/64)	0.876
H37Ra (1/128)	1.053

## 7- Figures

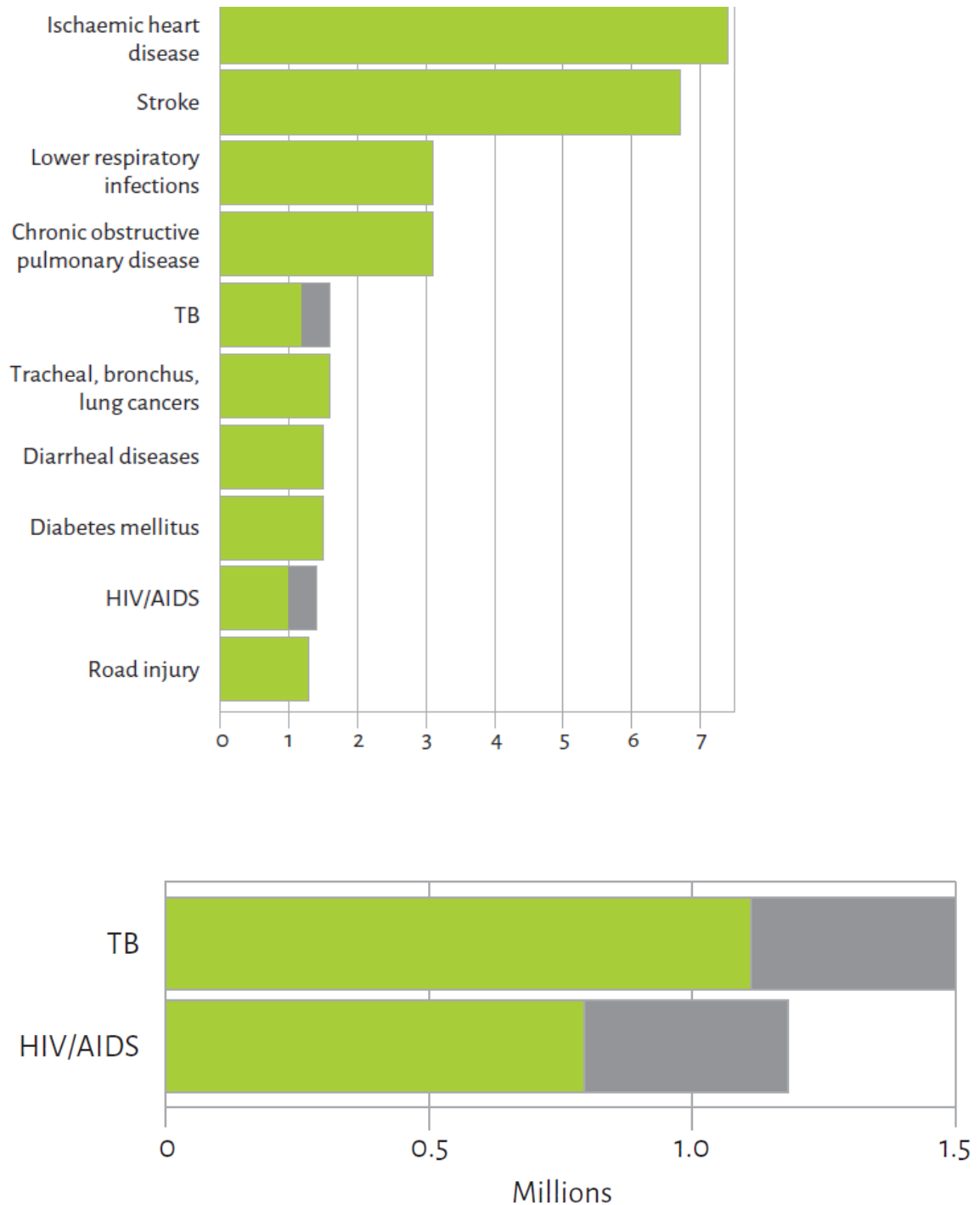


**Figure 1. Top causes of deaths worldwide.** Deaths numbers are for 2012 (on the top) and for 2014 (on the bottom). The gray part is the deaths due to HIV. The TB rate was 1.5 million people while the HIV rate was 1.2 million. Retrieved from [3].

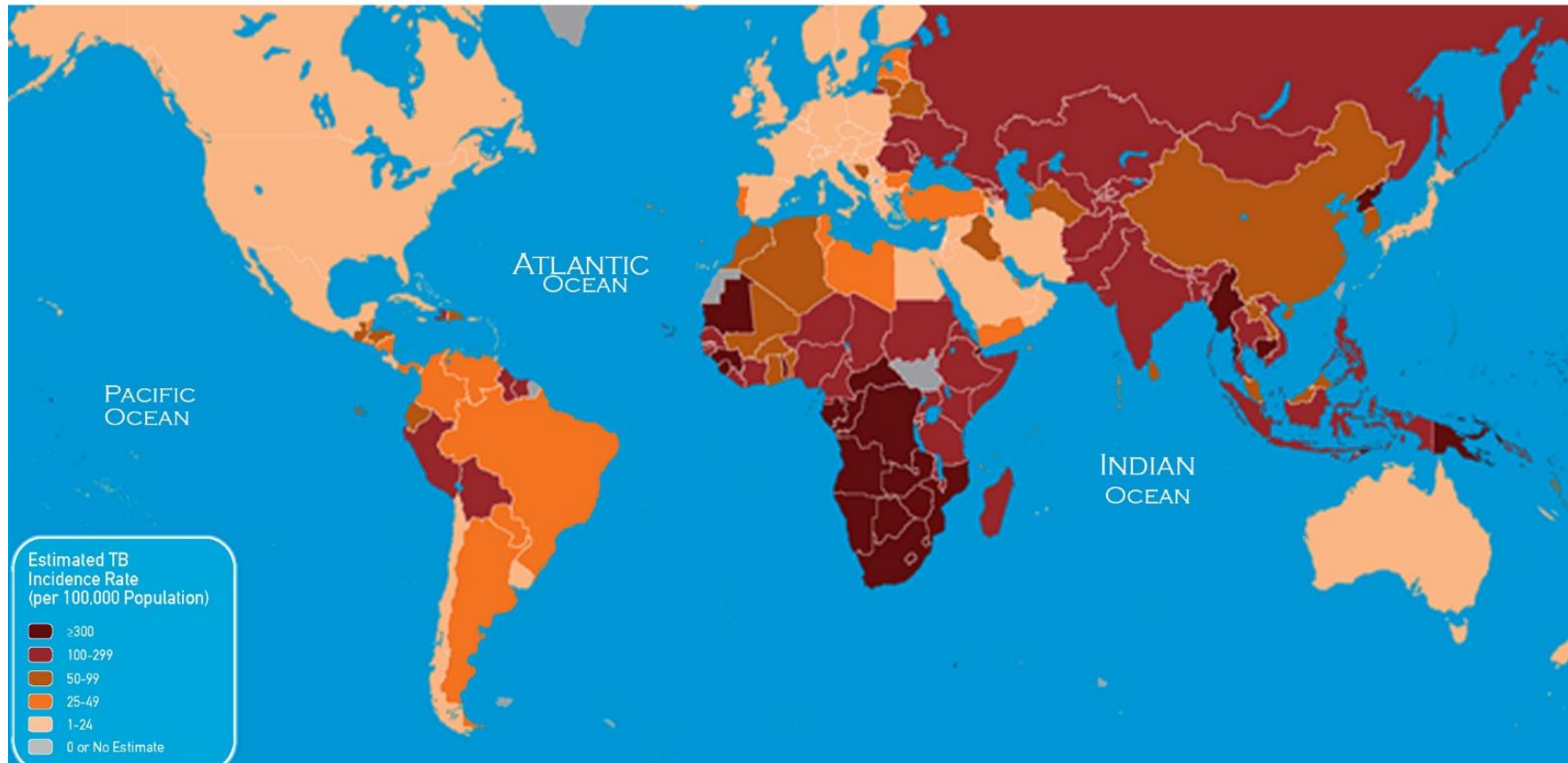


**Figure 2. The incidence of TB worldwide in 2014.** The number of TB patients and their geographic distribution are shown in different colors according to the density. Retrieved from:

[http://www.cdc.gov/travel-static/yellowbook/2014/map\\_3-13.png](http://www.cdc.gov/travel-static/yellowbook/2014/map_3-13.png)

# Egypt

Population 2014

90 million

Estimates of TB burden * 2014	Number (thousands)	Rate (per 100 000 population)
Mortality (excludes HIV+TB)	0.22 (0.2-0.25)	0.25 (0.22-0.27)
Mortality (HIV+TB only)	0.043 (0.035-0.051)	0.05 (0.04-0.06)
Prevalence (includes HIV+TB)	23 (12-37)	26 (13-42)
Incidence (includes HIV+TB)	13 (12-15)	15 (13-16)
Incidence (HIV+TB only)	0.035 (0.028-0.044)	0.04 (0.03-0.05)

Case detection, all forms (%)	54 (49-60)
-------------------------------	------------

Estimates of MDR-TB burden * 2014	New	Retreatment
% of TB cases with MDR-TB	3.4 (1.9-4.9)	15 (12-18)
MDR-TB cases among notified pulmonary TB cases	160 (87-220)	89 (72-110)

TB case notifications 2014	New **	Relapse
Pulmonary, bacteriologically confirmed	3 697	309
Pulmonary, clinically diagnosed	886	0
Extrapulmonary	2 285	0

<b>Total new and relapse</b>	<b>7 177</b>
Previously treated, excluding relapses	250
<b>Total cases notified</b>	<b>7 467</b>

Among 6 868 new cases:  
429 (6%) cases aged under 15 years; male:female ratio: 1.4

## Tuberculosis profile

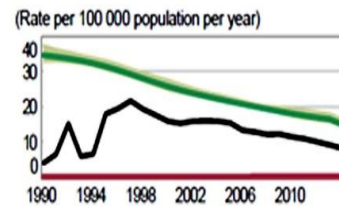
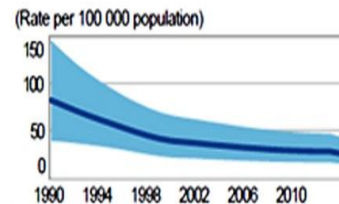
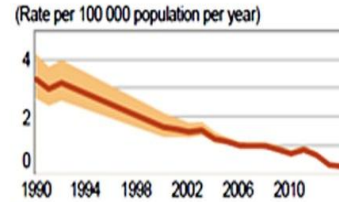


**Figure 3. Tuberculosis Egypt profile.** The figure is showing the incidence, prevalence and mortality rate of TB, MDR-TB and HIV patients with TB. Figure retrieved from [4].

## *Mycobacterium tuberculosis*

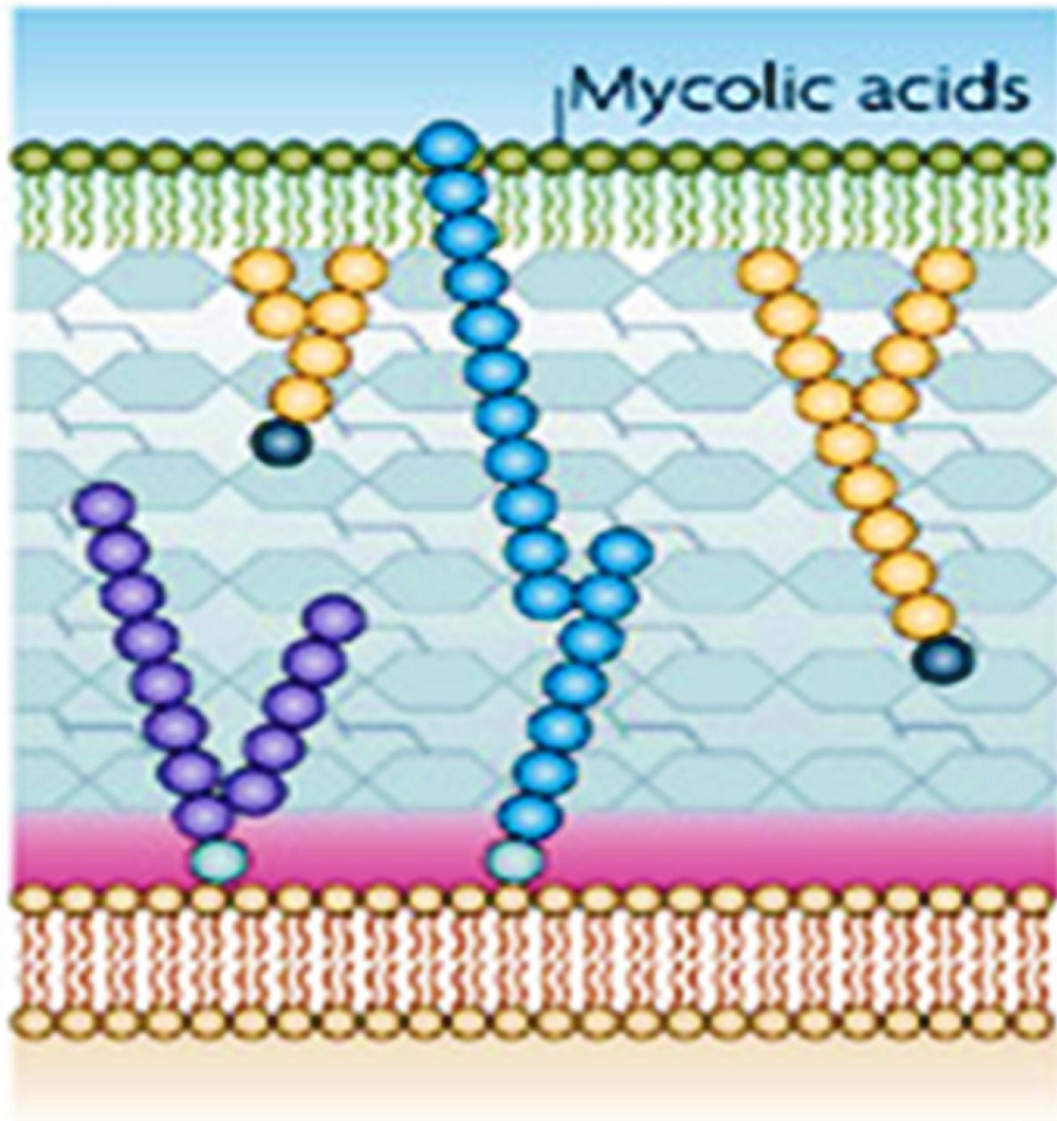


**Figure 4. The cell wall of MTB.** The mycolic acids appears attached to the peptidoglycan in the cell wall of MTB bacilli. Retrieved from <http://www.nature.com/nrmicro/journal/v6/n4/images/nrmicro1861-f1.jpg>



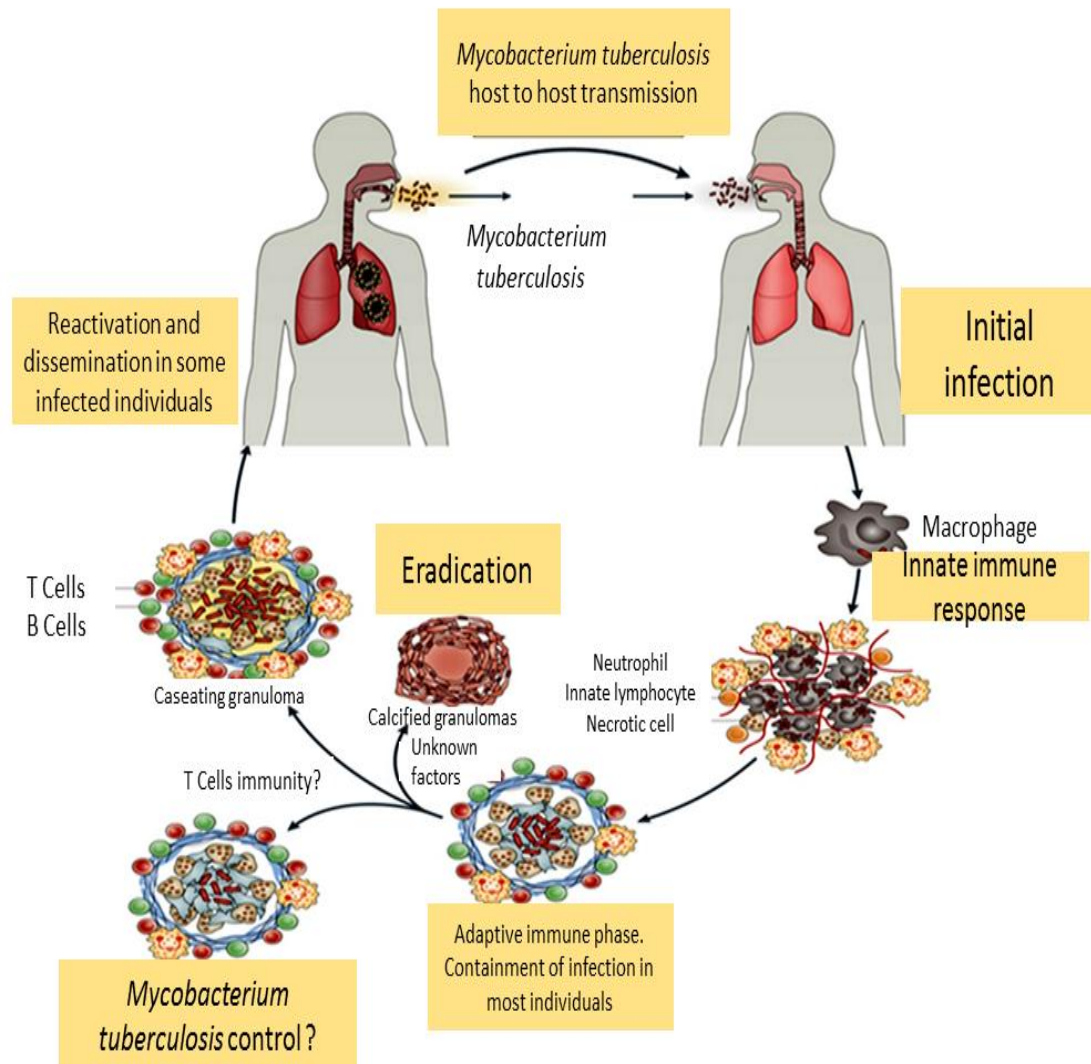


**Figure 5. The pathophysiology of MTB inside the host.** After inhalation of MTB bacilli and in case of healthy person, some bacilli may sneak to the lower respiratory tract. The macrophages hurry to the site of infection and destroy the bacilli. In case of the failure of the macrophages to terminate the bacteria, the macrophages engulf the bacilli forming Ghon complex. If the host's immunity becomes weaker, this granuloma may soften and the bacteria spread to the lung and other organs as the lymph nodes resulting in active infection. Retrieved from: <http://www.nature.com/nrmicro/journal/v12/n4/images/nrmicro3230-f1.jpg>

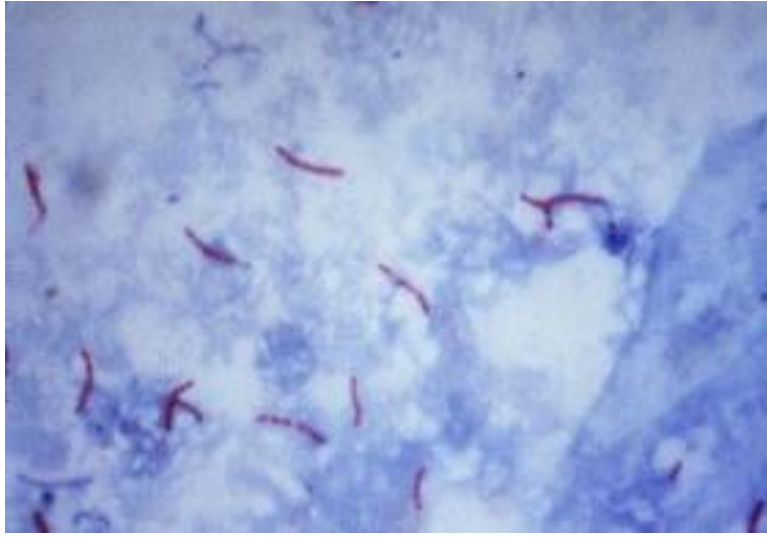


**Figure 6. The MTB bacilli after ZN staining under the microscope.** The bacilli appear as red rods under a blue background. Retrieved from [http://commons.wikimedia.org/wiki/File:Mycobacterium\\_tuberculosis\\_Ziehl-Neelsen\\_stain\\_02.jpg](http://commons.wikimedia.org/wiki/File:Mycobacterium_tuberculosis_Ziehl-Neelsen_stain_02.jpg)

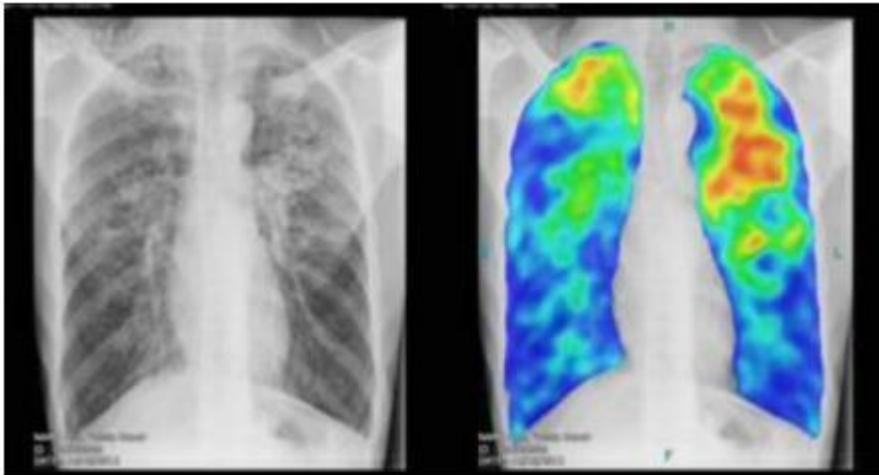


**Figure 7. Digital chest X-ray.** The left image is for digital chest X-ray. The right image is for CAD4TB analysis (specific software analyzes the images to detect any lung abnormalities) of the image. Both images show lung abnormalities. Retrieved from [24].



**Figure 8. Tuberculin assay.** The irritation is due to reaction with the injected antigen. After 48 hours, the injection site is tested. If the diameter of the injection site exceeded 10 mm in high risk people as infants, nurses, prisoners or HIV co-infected patients, this indicates TB active infection. If the diameter was 15 mm or more and there are no risk factors, this indicates active TB infection. Retrieved from: [http://www.healthcentral.com/common/images/9/9231\\_18546\\_5.jpg](http://www.healthcentral.com/common/images/9/9231_18546_5.jpg)

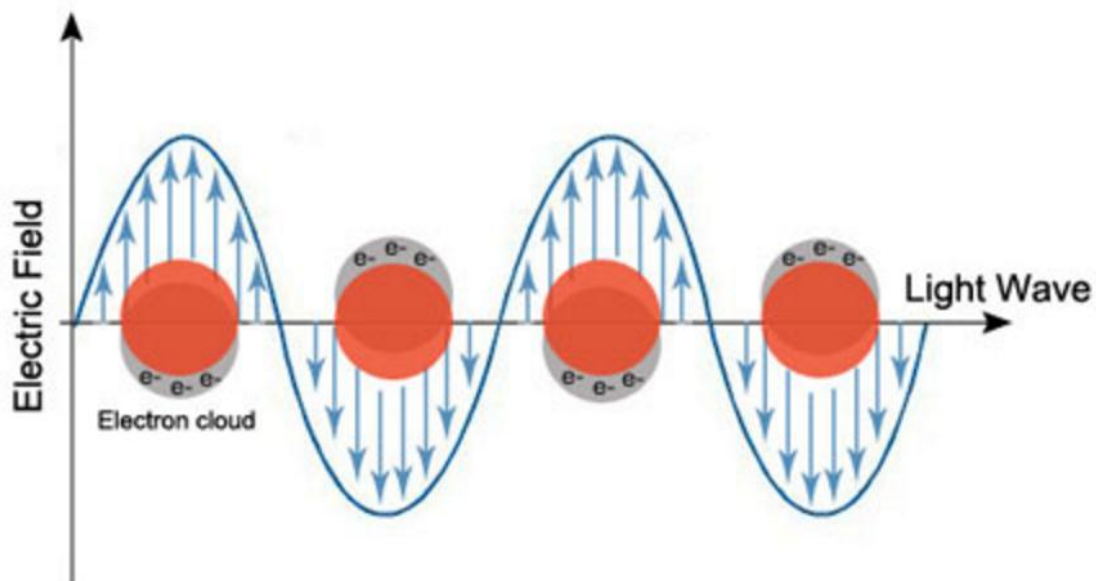


**Figure 9. The Surface Plasmon resonance of AuNPs.** When light with an electromagnetic field of a wavelength larger than AuNPs diameter hits the AuNPs, the nanoparticles induce a collective dipolar oscillation for the free electrons in the conduction around the metal nanoparticles surface. When these oscillations reach the maximum, this phenomenon is known as Surface Plasmon Resonance

Retrieved from:  
[http://pubs.rsc.org/services/images/RSCpubs.ePlatform.Service.FreeContent.ImageService.svc/ImageService/ArticleImage/2015/RA/c5ra01819f/c5ra01819f-f1\\_hi-res.gif](http://pubs.rsc.org/services/images/RSCpubs.ePlatform.Service.FreeContent.ImageService.svc/ImageService/ArticleImage/2015/RA/c5ra01819f/c5ra01819f-f1_hi-res.gif)

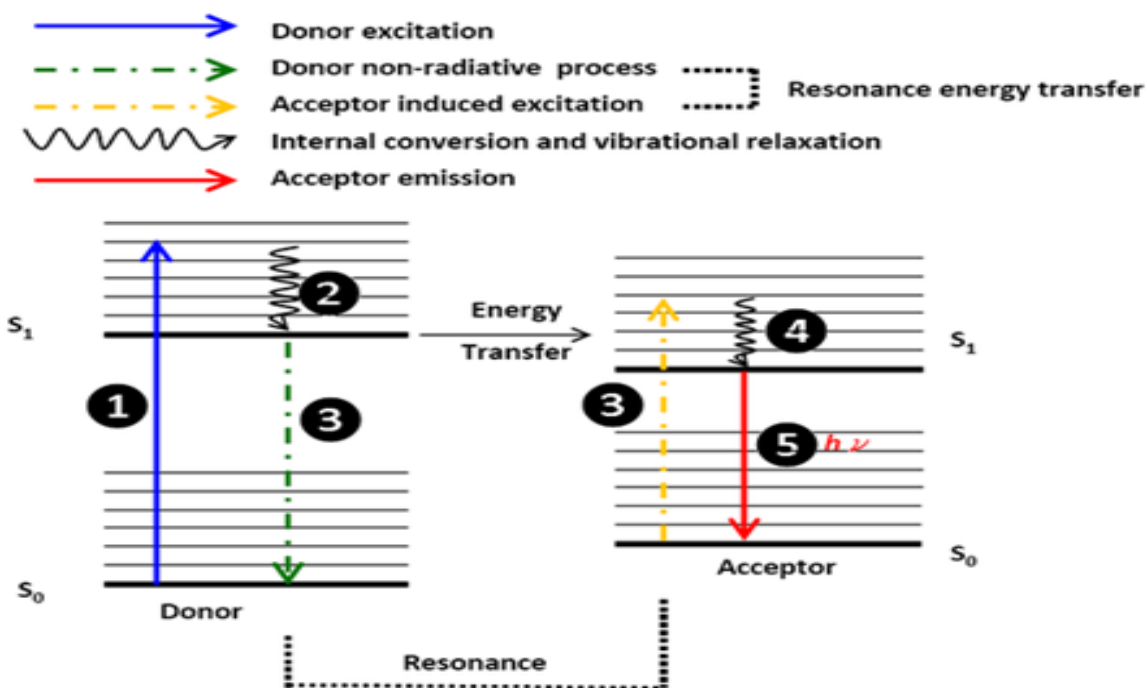


**Figure 10. The FRET energy transfer.** The donor is excited by a certain wave length. When the donor loses this energy as non-radiative energy, it transfers to the acceptor if it is present in the proper distance (not less than 7 nm) that allows energy transfer. The non-radiative energy transfer is called resonance.

- 1- Excitation of the donor by a photon from the ground state ( $S_0$ ) to the lowest excited state ( $S_1$ ).
- 2- Energy photon release of the donor and returning to the ground energy state
- 3- Energy transfer from the donor to the acceptor and excitation of the acceptor
- 4- Release of photon from the acceptor
- 5- Energy release of the acceptor to the ground energy state

Retrieved from:

[http://chemwiki.ucdavis.edu/Theoretical\\_Chemistry/Fundamentals/Fluorescence\\_Resonance\\_Energy\\_Transfer](http://chemwiki.ucdavis.edu/Theoretical_Chemistry/Fundamentals/Fluorescence_Resonance_Energy_Transfer)

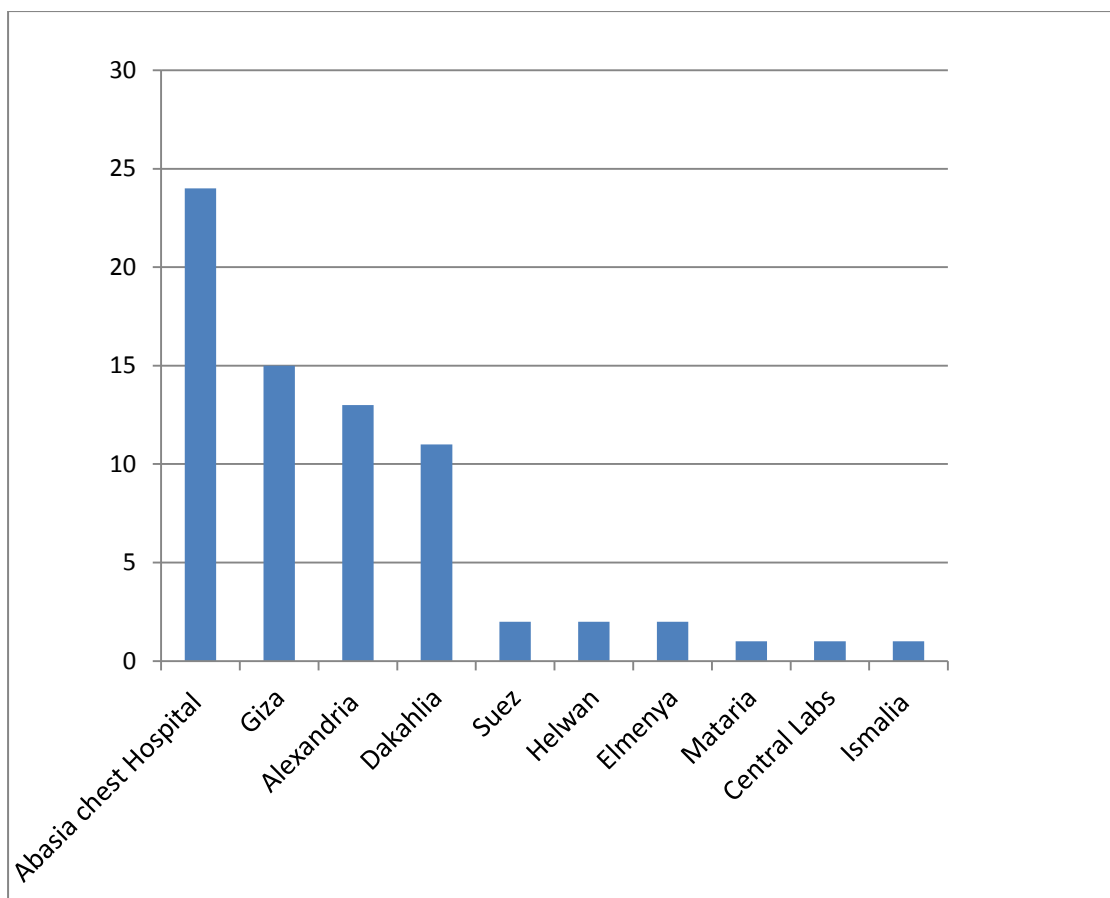


**Figure 11. Geographic distribution of the samples collected in Egypt.** The anonymous samples were obtained from patients of different geographic locations.

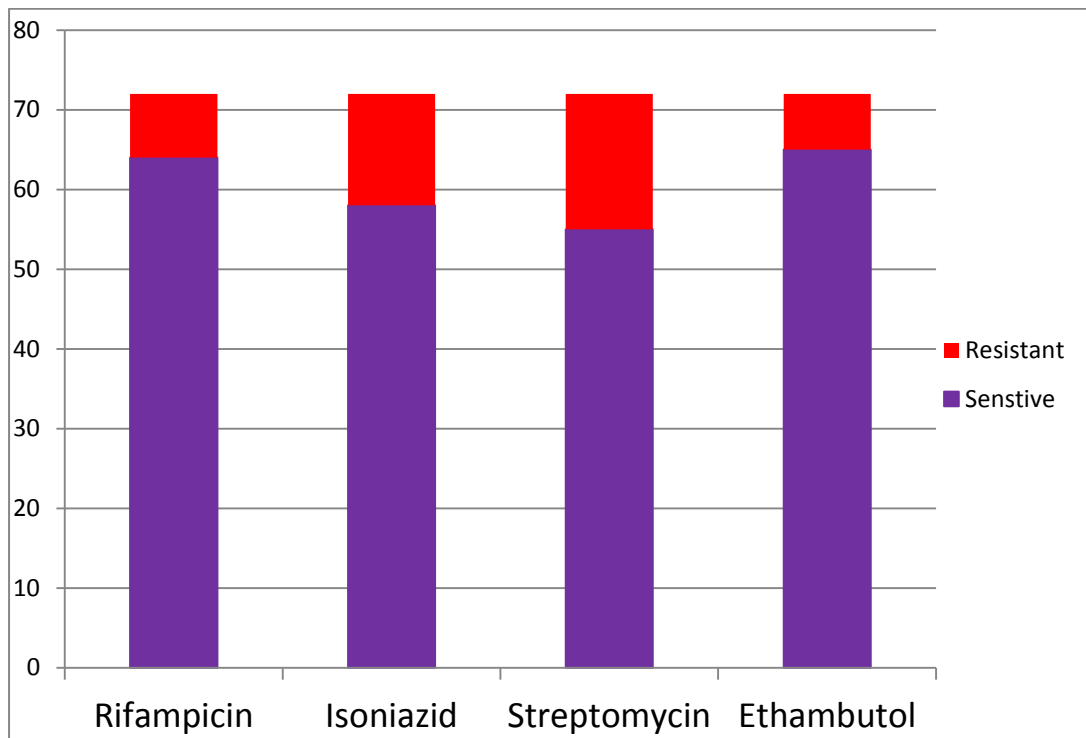


**Figure 12. Drug sensitivity results as obtained by culture.** The sensitivity of the first line antibiotics was investigated by culture in the Central Laboratories



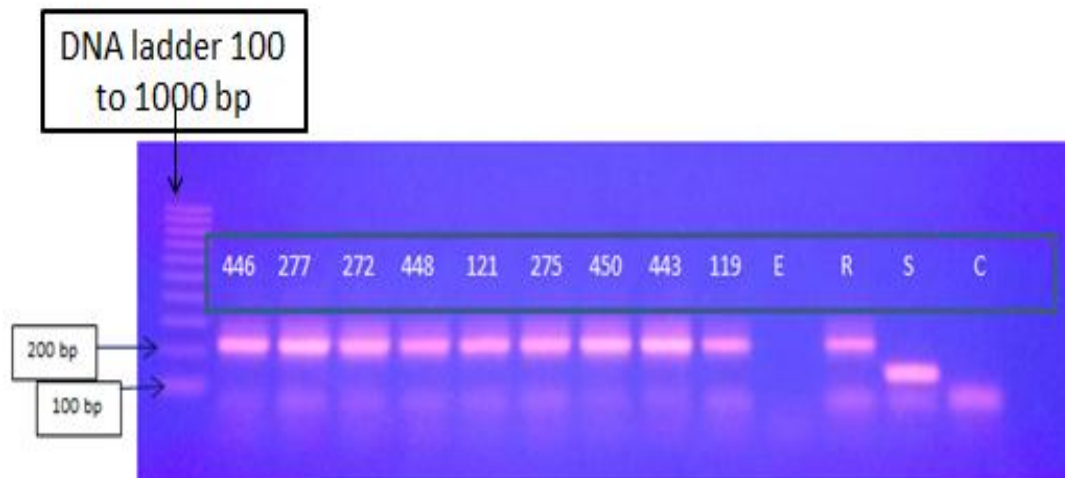


**Figure 13. Gel electrophoresis of multiplex PCR of mycobacterial samples.** The amplicons were investigated on 1.5% agarose gel stained with ethidium bromide and visualized by UV. Samples 446, 277, 272, 448, 121, 275, 450, 443 and 119 were proven to be MTB because the bands appeared at 235 bp. R: MTB H37Ra is the reference strain and had a band at 235 bp. S: *M. Smegmatis* which is NTM had a band at 136 bp. E: is *E.coli* sample did not have any band and c: control is just a blank by water instead of the sample.

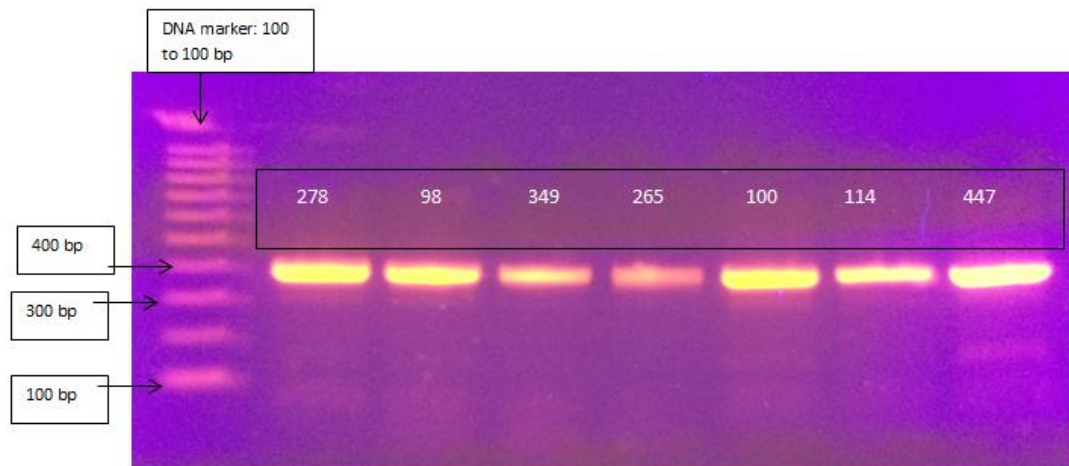


**Figure 14. PCR amplification of randomly chosen samples by 16S-23S ITS primers.** The randomly chosen samples were amplified and the amplicons were analyzed by 1.5% agarose gel stained with ethidium bromide. All the bands appeared at 350 which only verify the amplification but do not allow differentiation of the different species. The amplicons were then sequenced.

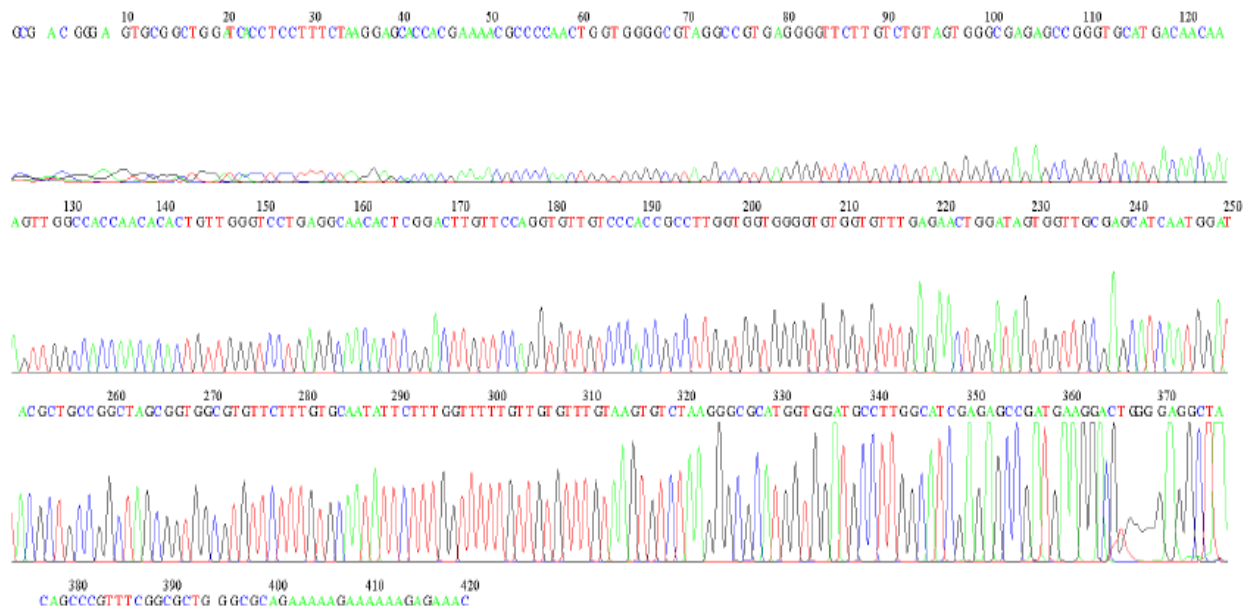


**Figure 15. Sequencing peaks of sample 300.** After the samples were amplified by 16S-23S ITS primers, the amplicons were purified and subjected to forward and reverse primer walking sequencing by Macrogen, South Korea.

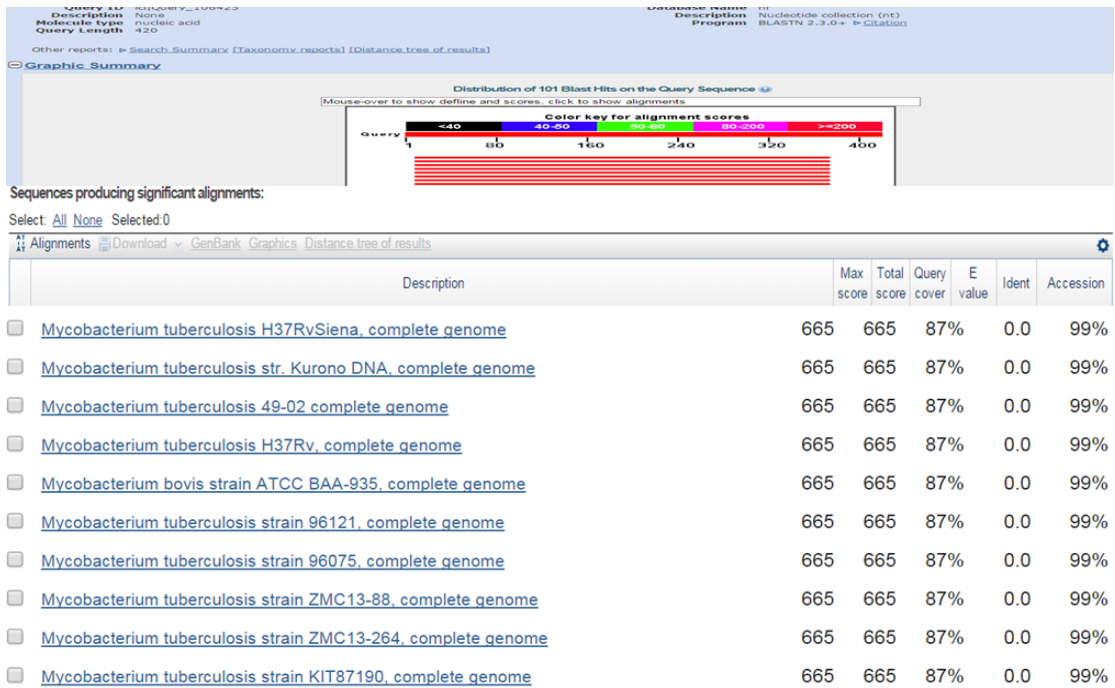


**Figure 16. NCBI BLAST analysis of sample 300.** After assembling of the forward and reverse sequences, the NCBI analysis was done.

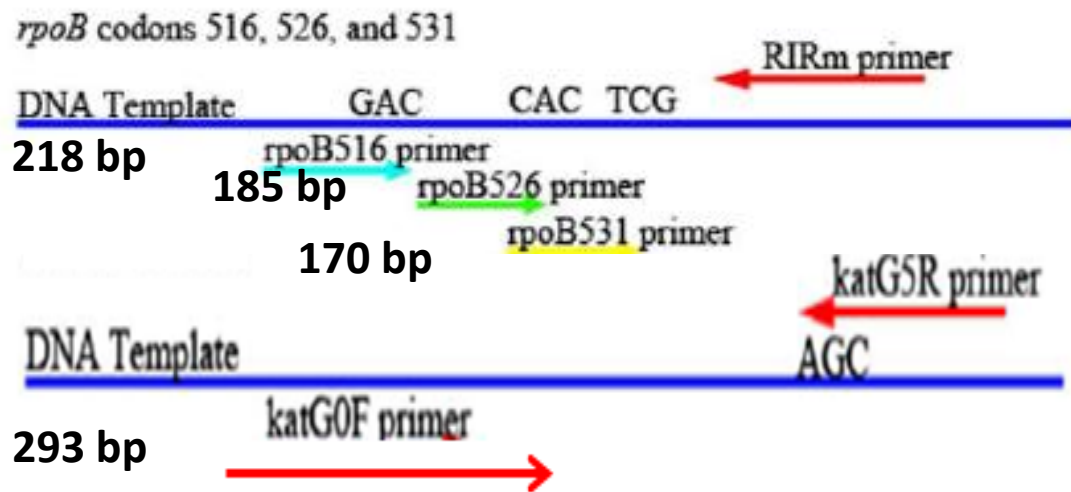


**Figure 17. Primers sites for amplification of MTB mutation sites.** Only wild type allows amplification and mutated types do not yield any amplicons. Figure retrieved from [81].

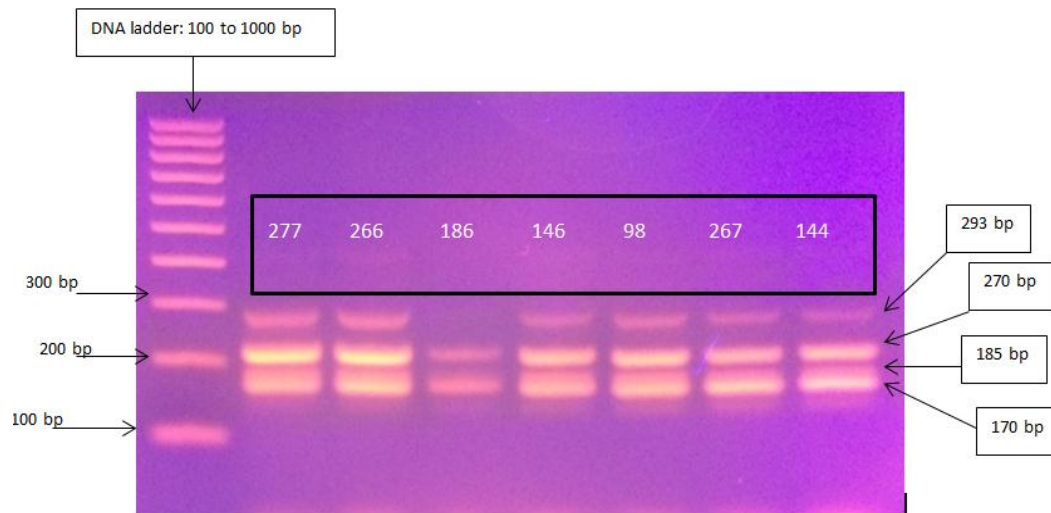


**Figure 18. Gel electrophoresis of MAS PCR of Mycobacterial samples.** Sample 186 was proven to be rifampicin resistant by culture, by PCR, the band at 170 bp was absent which means that rifampicin resistance is due to mutation in *rpoB* gene at 531 bp. Sample 267 was Isoniazid resistant by culture. However, the resistance was probably due to other mutation rather than *KatG* gene.

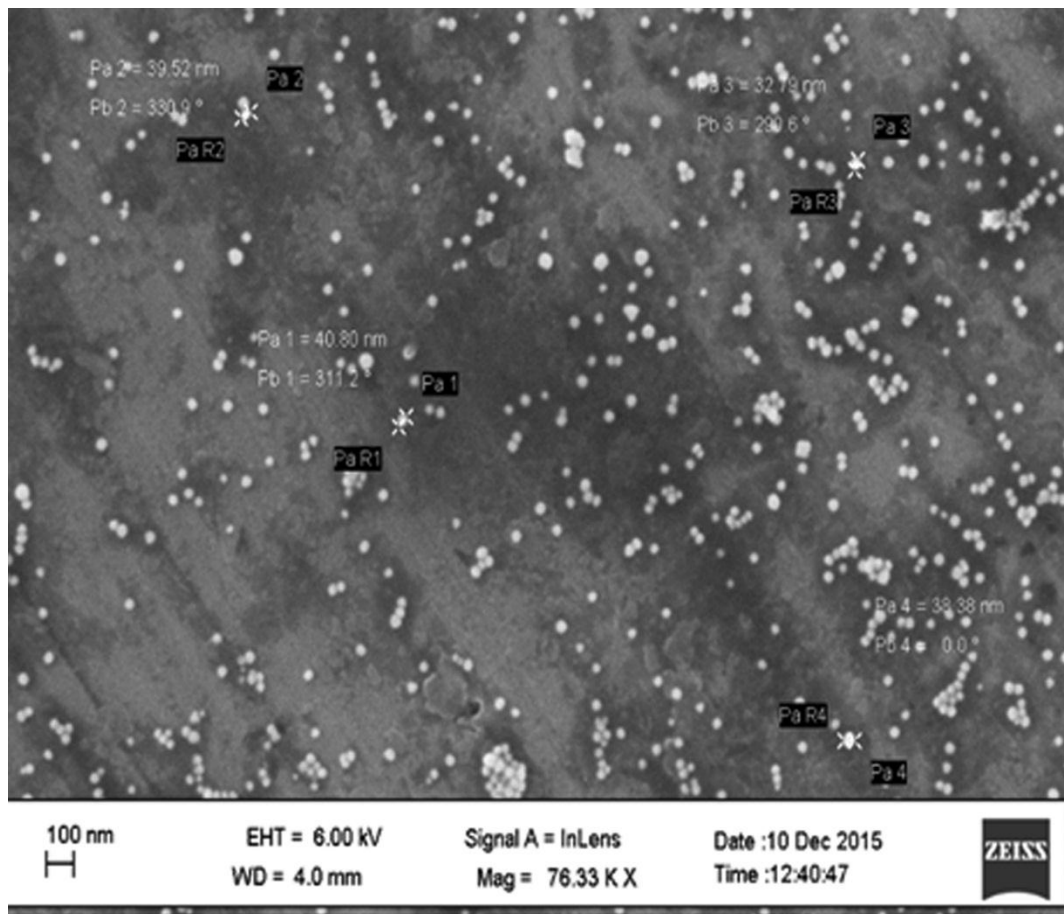


**Figure 19. Anionic AuNPs characterization by SEM.** After preparation of the AuNPs without concentration, 10  $\mu$ l are allowed to dry on aluminum foil covering a glass slide. After complete dryness of the AuNPs, investigation is performed by SEM. The particles are spherical, of nearly uniform size and the average diameter is 40 nm.

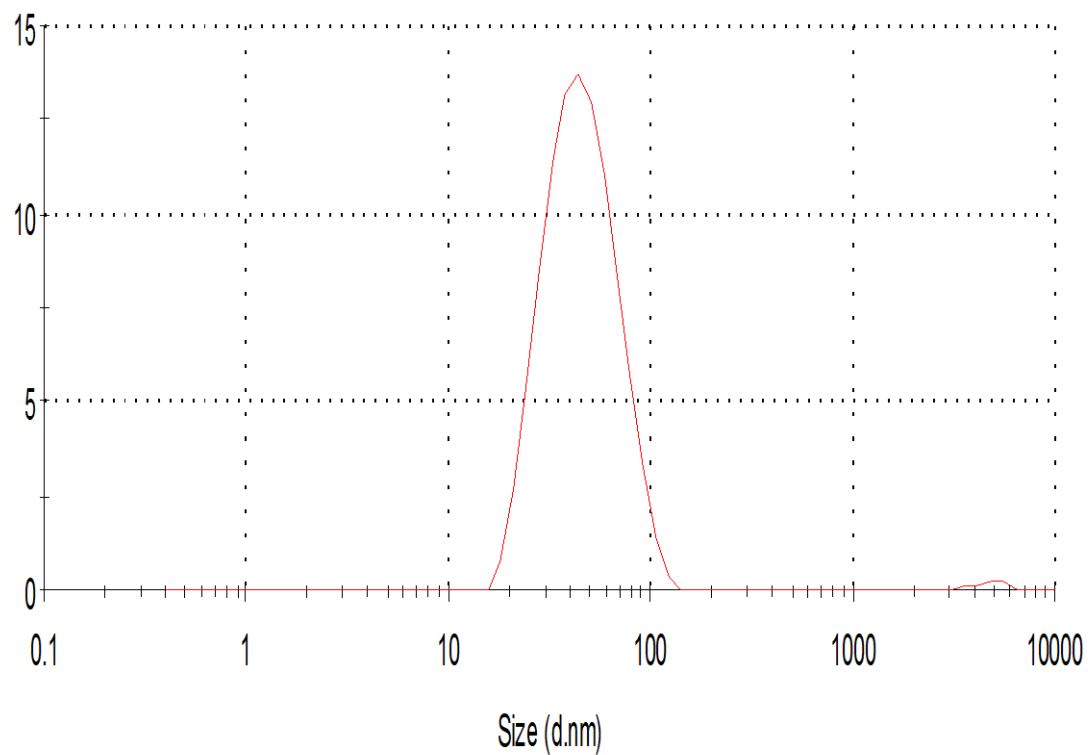


**Figure 20. Anionic AuNPs characterization by zeta sizer.** After preparing the AuNPs without concentration, 100  $\mu\text{l}$  of the AuNPs are added to 1900  $\mu\text{l}$  NFW and then fill the cuvette from this dilution. The peak is at 40 nm.



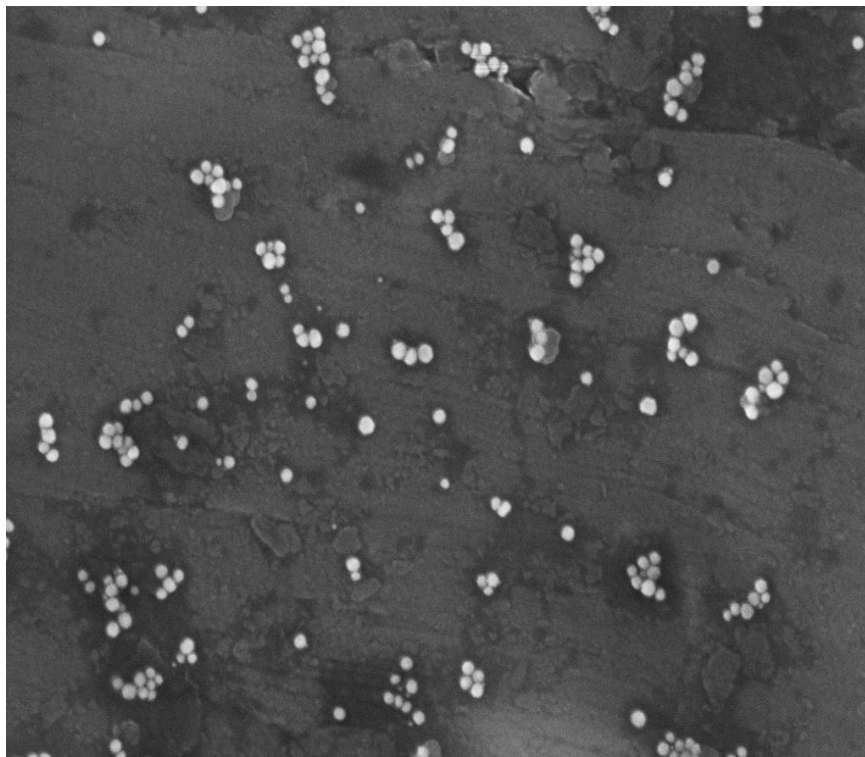


**Figure 21. SEM imaging of cationic AuNPs.** After preparation of the AuNPs without concentration, 10  $\mu\text{l}$  are allowed to dry on aluminum foil covering a glass slide. After complete dryness of the AuNPs, investigation is performed by SEM. The particles are of uniform shape and diameter. The average diameter is 20 nm.

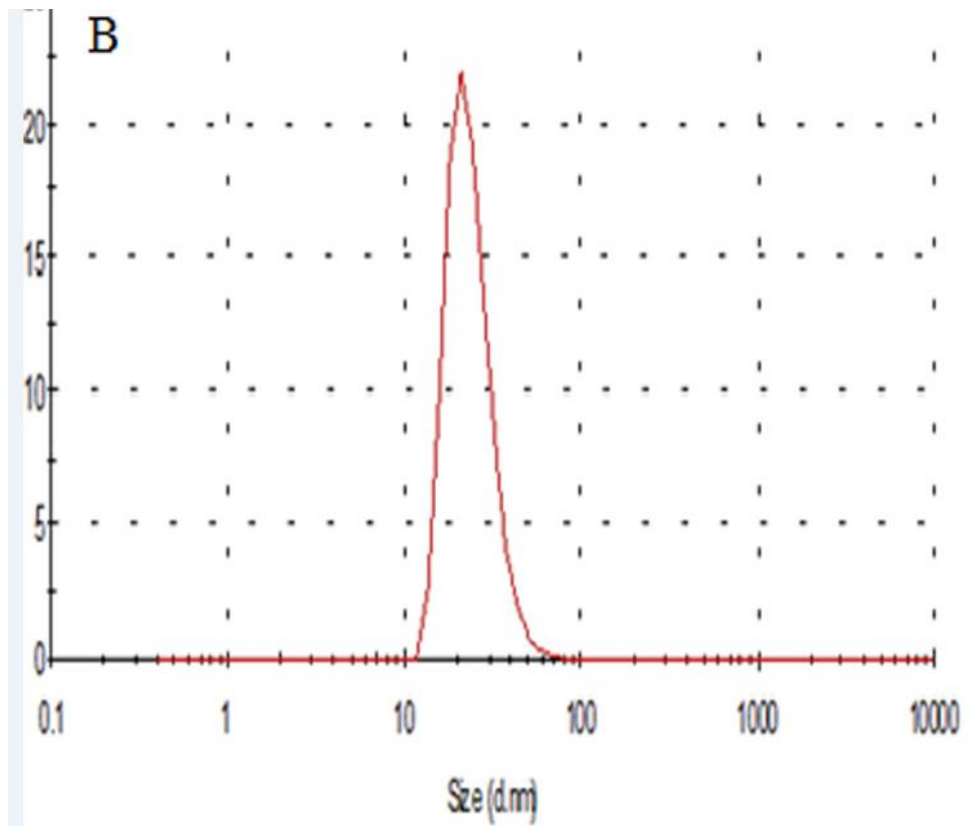


**Figure 22. Zeta size characterization of cationic AuNPs.** After preparing AuNPs without concentration, 100  $\mu\text{l}$  of the AuNPs are added to 1900  $\mu\text{l}$  NFW and then fill the cuvette from this dilution. The peak is at 20 nm.

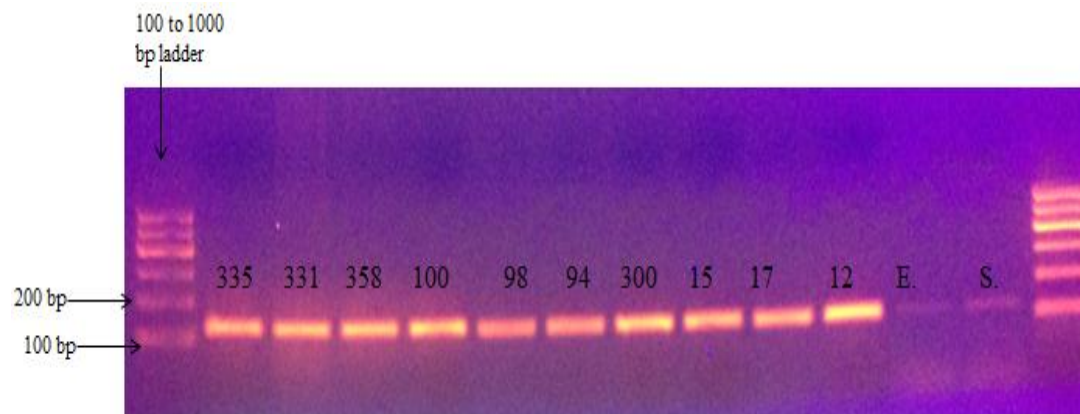


**Figure 23. Gel electrophoresis of *IS6110* amplification of bacterial strains.** Samples 335, 331, 358, 100, 98, 94, 300, 15, 17 and 12 are *Mycobacterium tuberculosis* samples and yielded bands at 123 bp, *E. coli* (E) sample and *M. smegmatis* (S) sample did not have any bands because they lack the amplified sequence.

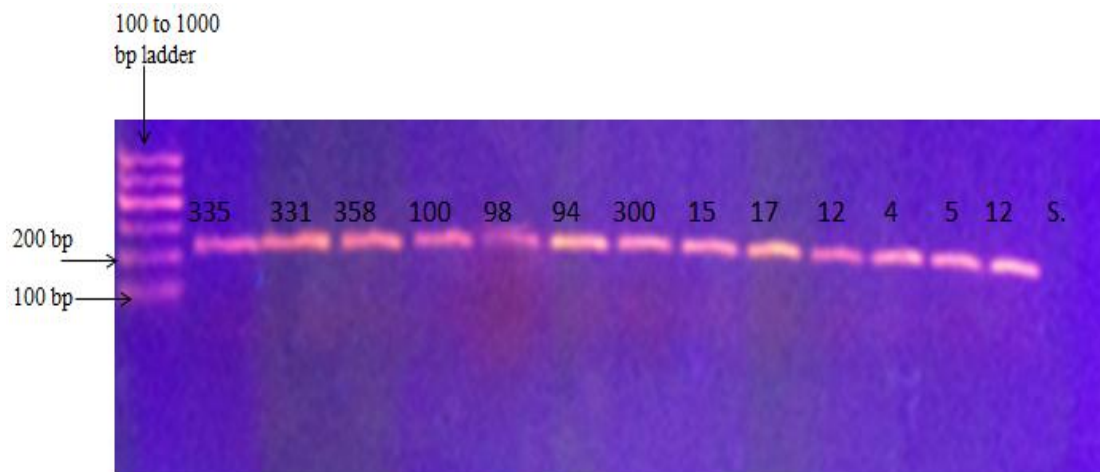


**Figure 24. Gel electrophoresis of *rpoB* amplification of bacterial strains:** samples 335, 331, 358, 100, 98, 94, 300, 15, 17, 12, 4, 5 and 12 are *Mycobacterium tuberculosis* samples and yielded bands at 235 bp. *M. smegmatis* (S) did not yield any band.

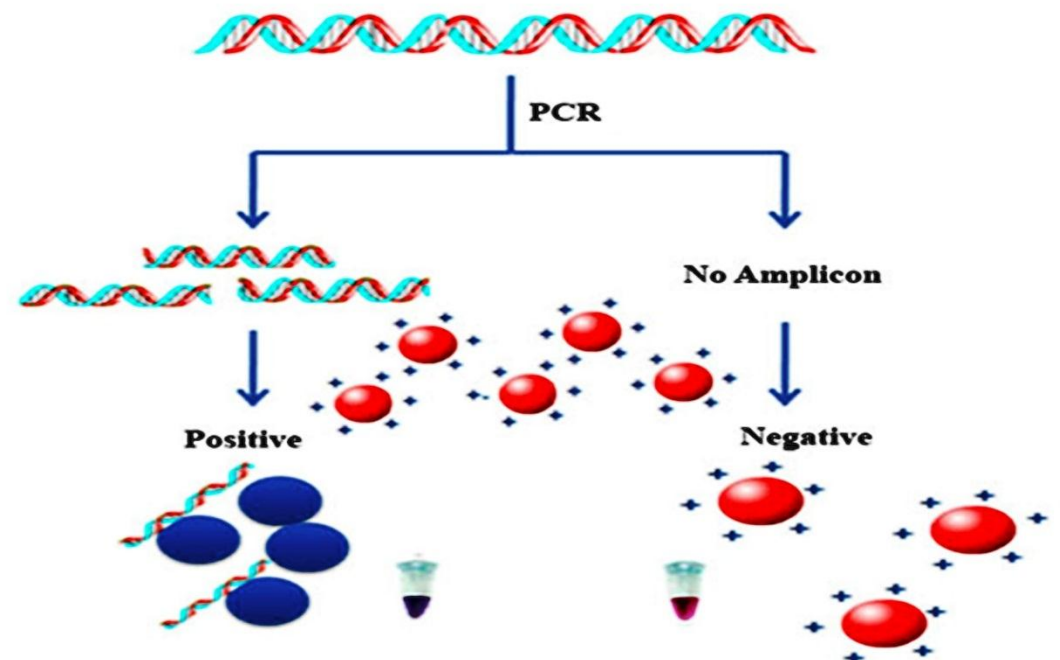


**Figure 25. Diagram for Cationic AuNPs assay.** In the case of positive samples, the presence of the target DNA sequence resulted in formation of amplified DNA product. The negative DNA charge will attract the positively charged AuNPs leading to their aggregation and thus the appearance of the blue color. However, in case of negative samples, no PCR product formed and the AuNPs remain dispersed. The repulsion forces between the AuNPs keep the intra-particles distances constant, subsequently, the colloidal color remains red. Azzazy ©.



**Figure 26. Cationic AuNPs assay of *rpoB* amplicons of MTB DNA samples. 335, 358, 331, 100 and 98. S: *M. smegmatis* sample.** The MTB samples were amplified by the *rpoB* primers then cationic AuNPs were added to the amplicons. The attraction between the negatively charged amplicons and the positively charged AuNPs induced the color from red to violet due to the AuNPs aggregation. The *M. smegmatis* was not amplified because it lacks the complementary sequences for the primers hybridization so the AuNPs remained dispersed.

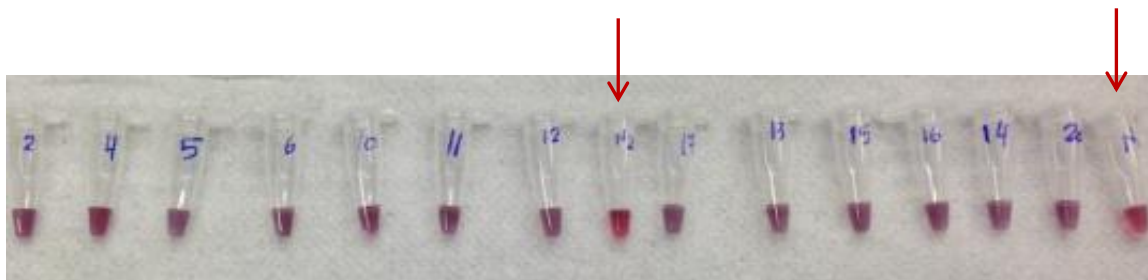


**Figure 27. Cationic AuNPs assay of *IS6110* amplicons of MTB DNA samples:** 2, 4, 5, 6, 10, 11, 12, NI (*M. smegmatis* sample, pointed by red arrow), 17, 13, 15, 16, 14, 20, N2 (*E. coli* sample, pointed by red arrow). The numbered samples are MTB samples and thus the tubes turned blue. The MTB samples were amplified by the *IS6110* primers then cationic AuNPs were added to the amplicons. The attraction between the negatively charged amplicons and the positively charged AuNPs induced the color from red to violet due to the AuNPs aggregation. The *M. smegmatis* was not amplified because it lacks the complementary sequences for the primers hybridization so the AuNPs remained dispersed.

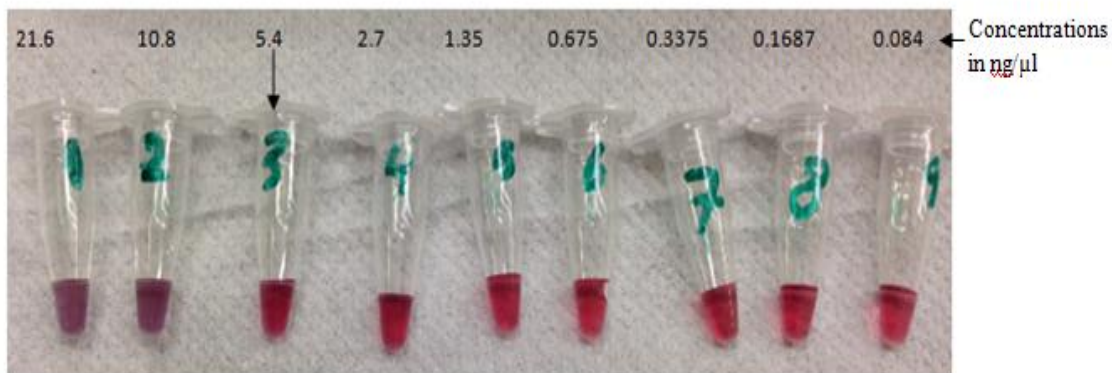


**Figure 28. Detection limit by Cationic AuNPs assay of *IS6110* amplicons.** Serial dilutions were prepared and investigated. The initial DNA concentration was calculated after measuring absorption at 260 and 280 nm. The detection limit was the least amount of DNA induced color change and was found to be 5.4 ng/μl.



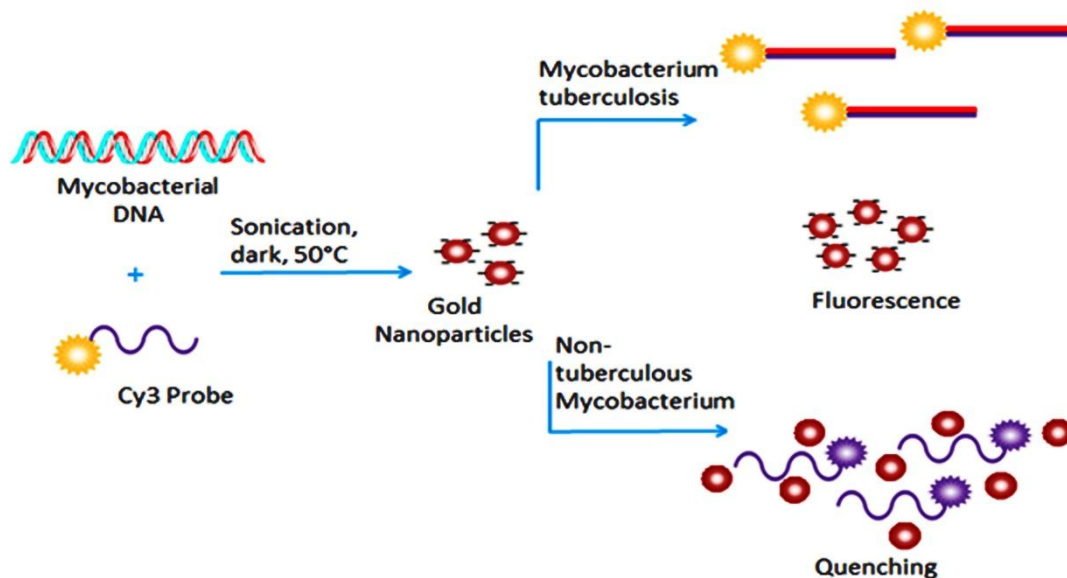


**Figure 29. Diagram for FRET assay.** In presence of the target in case of MTB DNA, the probe hybridizes with the CY3-16s rDNA specific probe; the more stable dsDNA structure is formed. This exposes the negatively charged phosphate backbone to the outer media where the negatively charged AuNPs are present; resulting in repulsion and adsorption of the AuNPs to the DNA is prevented. Consequently, the gold nanoparticle is spaced from CY-3 and fluorescence is emitted. In absence of the target as in the *M. smegmatis* and the negative controls, the AuNPs become in close proximity to the CY-3 probe. Azzazy ©.

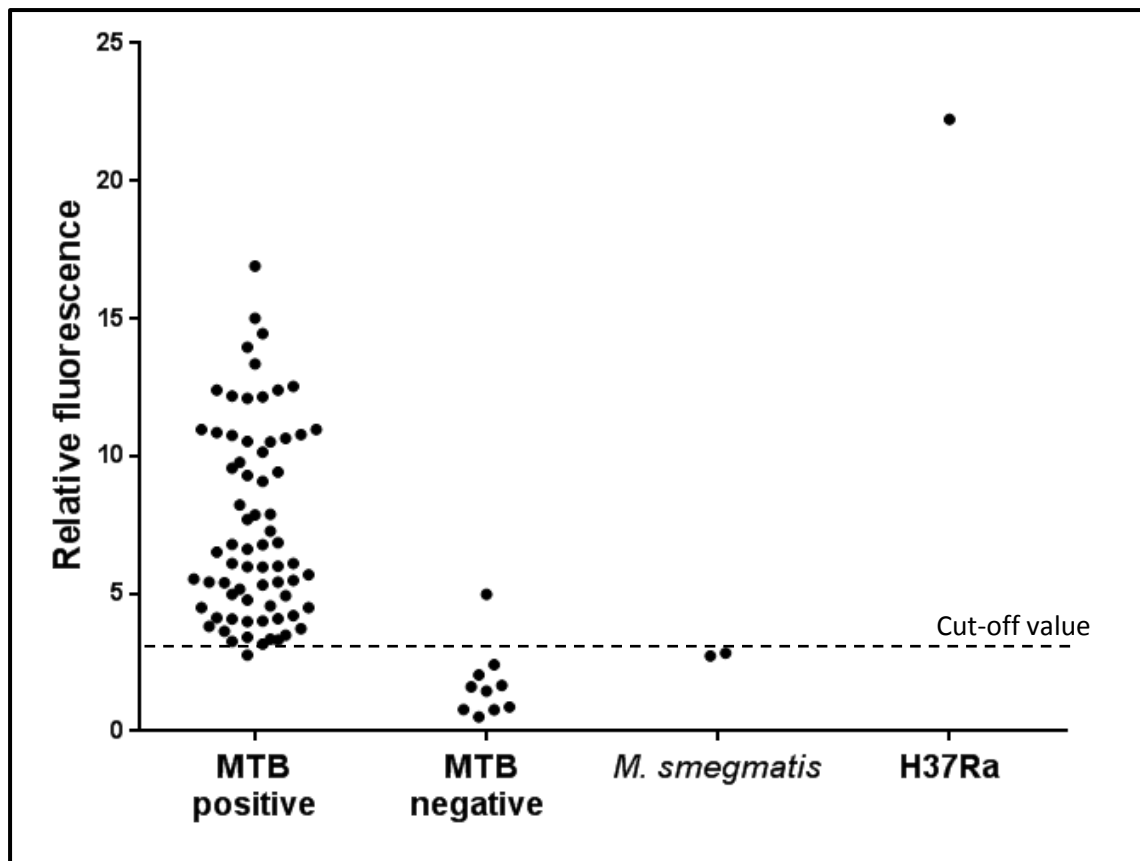


**Figure 30. FRET results by CY-3 16s rDNA specific probe.** The MTB samples were above the cut-off value which is 3 folds the negative control value. The *M. smegmatis* and the negative samples were under the cut-off value.

## **Acknowledgement**

This thesis was made possible by a NPRP award [NPRP 4 - 1215 - 3 - 317] from the Qatar National Research Fund (a member of The Qatar Foundation) awarded to Professor Hassan Azzazy. The statements made herein are solely the responsibility of the authors.

## 8- References

1. Smith, I., *Mycobacterium tuberculosis pathogenesis and molecular determinants of virulence*. Clinical Microbiology Reviews, 2003. **16**(3): p. 463-496.
2. Da Silva, P.E.A. and J.C. Palomino, *Molecular basis and mechanisms of drug resistance in Mycobacterium tuberculosis: classical and new drugs*. Journal of Antimicrobial Chemotherapy, 2011. **66**(7): p. 1417-1430.
3. World Health Organization, *Global tuberculosis report 2015*. 2015.
4. World Health Organization., *Country Profiles 2011*. 2011.
5. Mutingwende, I., et al., *Development and evaluation of a rapid multiplex-PCR based system for Mycobacterium tuberculosis diagnosis using sputum samples*. Journal of Microbiological Methods, 2015. **116**: p. 37-43.
6. Hazbón, M.H., *Recent advances in molecular methods for early diagnosis of tuberculosis and drug-resistant tuberculosis*. Biomedica, 2004. **24**: p. 149-162.
7. World Health Organization, *The global plan to stop TB 2011-2015: transforming the fight towards elimination of tuberculosis*. 2010.
8. World Health Organization, *An international roadmap for tuberculosis research: towards a world free of tuberculosis*. Geneva: WHO, 2011.
9. Jagielski, T., et al., *Current methods in the molecular typing of Mycobacterium tuberculosis and other mycobacteria*. BioMed Research International, 2014. **2014**.
10. Neonakis, I.K., et al., *Molecular diagnostic tools in mycobacteriology*. Journal of Microbiological Methods, 2008. **75**(1): p. 1-11.
11. Fu, L. and C. Fu-Liu, *Is Mycobacterium tuberculosis a closer relative to Gram-positive or Gram-negative bacterial pathogens?* Tuberculosis, 2002. **82**(2): p. 85-90.
12. WEST, P., *MICROBIOLOGY-AN INTRODUCTION-TORTORA, GJ, FUNKE, BR, CASE, CL*. 1983, UNIV CHICAGO PRESS 5720 S WOODLAWN AVE, CHICAGO, IL 60637.

13. Korf, J., et al., *The Mycobacterium tuberculosis cell wall component mycolic acid elicits pathogen-associated host innate immune responses*. European Journal of Immunology, 2005. **35**(3): p. 890-900.
14. Brennan, P.J., *Structure, function, and biogenesis of the cell wall of Mycobacterium tuberculosis*. Tuberculosis, 2003. **83**(1): p. 91-97.
15. Velayati, A.A. and P. Farnia, *Morphological Characterization of Mycobacterium tuberculosis*. 2012: INTECH Open Access Publisher.
16. Lorenzo, D. and S.A. Mousa, *Mechanisms of drug resistance in Mycobacterium tuberculosis and current status of rapid molecular diagnostic testing*. Acta Tropica, 2011. **119**(1): p. 5-10.
17. Yao, C., et al., *Detection of rpoB, katG and inhA gene mutations in Mycobacterium tuberculosis clinical isolates from Chongqing as determined by microarray*. Clinical Microbiology and Infection, 2010. **16**(11): p. 1639-1643.
18. Parsons, L.M., et al., *Laboratory diagnostic aspects of drug resistant tuberculosis*. Front Biosci, 2004. **9**: p. 2086-2105.
19. Nakata, N., M. Kai, and M. Makino, *Mutation Analysis of Mycobacterial rpoB Genes and Rifampicin Resistance Using Recombinant Mycobacterium smegmatis*. Antimicrobial Agents and Chemotherapy, 2012: p. AAC. 05831-11.
20. Davies, P.D., *Multi-drug-resistant tuberculosis*, in *Tuberculosis*. 2004, Springer. p. 809-837.
21. Lemus, D., et al., *Nitrate reductase assay for detection of drug resistance in Mycobacterium tuberculosis: simple and inexpensive method for low-resource laboratories*. Journal of Medical Microbiology, 2006. **55**(7): p. 861-863.
22. Kocagöz, T., et al., *Detection of Mycobacterium tuberculosis in sputum samples by polymerase chain reaction using a simplified procedure*. Journal of Clinical Microbiology, 1993. **31**(6): p. 1435-1438.
23. Miller, L.P., J.T. Crawford, and T.M. Shinnick, *The rpoB gene of Mycobacterium tuberculosis*. Antimicrobial Agents and Chemotherapy, 1994. **38**(4): p. 805-811.
24. UNITAID, W., *Tuberculosis Diagnostic Technology and Market Landscape*. Geneva: World Health Organization, 2013.

25. Hashemi-Shahraki, A., et al., *Species spectrum of nontuberculous mycobacteria isolated from suspected tuberculosis patients, identification by multi locus sequence analysis*. Infection, Genetics and Evolution, 2013. **20**: p. 312-324.
26. Worodria, W., et al., *The role of speciation in positive lowenstein-jensen culture isolates from a high tuberculosis burden country*. PloS One, 2011. **6**(11): p. e27017.
27. Hwang, S.M., et al., *Simultaneous detection of Mycobacterium tuberculosis complex and nontuberculous mycobacteria in respiratory specimens*. Tuberculosis, 2013. **93**(6): p. 642-646.
28. Tsai, T.-T., et al., *Paper-based tuberculosis diagnostic devices with colorimetric gold nanoparticles*. Science and Technology of Advanced Materials, 2013. **14**(4): p. 044404.
29. Unitaid, *Tuberculosis diagnostic technology landscape 2012*. World Health Organization, 2012.
30. World Health Organization, *Policy framework for implementing new tuberculosis diagnostics*. Geneva: WHO, 2010.
31. Parsons, L.M., et al., *Laboratory diagnosis of tuberculosis in resource-poor countries: challenges and opportunities*. Clinical Microbiology Reviews, 2011. **24**(2): p. 314-350.
32. Steingart, K.R., et al., *Commercial serological tests for the diagnosis of active pulmonary and extrapulmonary tuberculosis: an updated systematic review and meta-analysis*. PLoS Medicine, 2011. **8**(8): p. 1063.
33. Metcalfe, J.Z., et al., *Interferon- $\gamma$  release assays for active pulmonary tuberculosis diagnosis in adults in low-and middle-income countries: systematic review and meta-analysis*. Journal of Infectious Diseases, 2011. **204**(suppl 4): p. S1120-S1129.
34. Mokaddas, E. and S. Ahmad, *Development and evaluation of a multiplex PCR for rapid detection and differentiation of Mycobacterium tuberculosis complex members from non-tuberculous mycobacteria*. Japanese Journal of Infectious Diseases, 2007. **60**(2/3): p. 140.
35. Wolinsky, E., *Conventional diagnostic methods for tuberculosis*. Clinical Infectious Diseases, 1994: p. 396-401.

36. Grange, J.M., et al., *Guidelines for speciation within the Mycobacterium tuberculosis complex*. 1996: WHO.
37. Niemann, S., E. Richter, and S. Rüscher-Gerdes, *Differentiation among Members of the Mycobacterium tuberculosis Complex by Molecular and Biochemical Features: Evidence for Two Pyrazinamide-Susceptible Subtypes of M. bovis*. *Journal of Clinical Microbiology*, 2000. **38**(1): p. 152-157.
38. Cheng, V.C.-C., W.W. Yew, and K.Y. Yuen, *Molecular diagnostics in tuberculosis*. *European Journal of Clinical Microbiology and Infectious Diseases*, 2005. **24**(11): p. 711-720.
39. Reddington, K., et al., *SeekTB, a two-stage multiplex real-time-PCR-based method for differentiation of the mycobacterium tuberculosis complex*. *Journal of Clinical Microbiology*, 2012. **50**(7): p. 2203-2206.
40. Oliphant, C.M., *Tuberculosis*. *The Journal for Nurse Practitioners*. **11**(1): p. 87-94.
41. World Health Organization, *Non-commercial culture and drug-susceptibility testing methods for screening of patients at risk of multidrug resistant tuberculosis*. 2010 Jul [cited 2011 Jan 20].
42. Sharma, B., et al., *Evaluation of a Rapid Differentiation Test for Mycobacterium Tuberculosis from other Mycobacteria by Selective Inhibition with p-nitrobenzoic Acid using MGIT 960*. *Journal of Laboratory Physicians*, 2010. **2**(2): p. 89-92.
43. Alva, A., et al., *Morphological characterization of Mycobacterium tuberculosis in a MODS culture for an automatic diagnostics through pattern recognition*. *Plos One*, 2013. e82809.
44. Gupta, A., et al., *Evaluation of the performance of nitrate reductase assay for rapid drug-susceptibility testing of Mycobacterium tuberculosis in north India*. *Journal of Health, Population and Nutrition*, 2011. **29**(1): p. 20.
45. Kocagöz, T., et al., *Efficiency of the TK Culture System in the diagnosis of tuberculosis*. *Diagnostic Microbiology and Infectious Disease*, 2012. **72**(4): p. 350-357.
46. Palomino, J. and F. Portaels, *Simple procedure for drug susceptibility testing of Mycobacterium tuberculosis using a commercial colorimetric assay*.

- European Journal of Clinical Microbiology and Infectious Diseases, 1999. **18**(5): p. 380-383.
47. Martin, A., F. Portaels, and J.C. Palomino, *Colorimetric redox-indicator methods for the rapid detection of multidrug resistance in Mycobacterium tuberculosis: a systematic review and meta-analysis*. Journal of Antimicrobial Chemotherapy, 2007. **59**(2): p. 175-183.
  48. Kumar, M., et al., *Rapid, inexpensive MIC determination of Mycobacterium tuberculosis isolates by using microplate nitrate reductase assay*. Diagnostic Microbiology and Infectious Disease, 2005. **53**(2): p. 121-124.
  49. Cho, S.-N., *Current issues on molecular and immunological diagnosis of tuberculosis*. Yonsei Medical Journal, 2007. **48**(3): p. 347-359.
  50. Drobniewski, F., et al., *A clinical, microbiological and economic analysis of a national service for the rapid molecular diagnosis of tuberculosis and rifampicin resistance in Mycobacterium tuberculosis*. Journal of Medical Microbiology, 2000. **49**(3): p. 271-278.
  51. Kaul, K.L., *Molecular detection of Mycobacterium tuberculosis: impact on patient care*. Clinical Chemistry, 2001. **47**(8): p. 1553-1558.
  52. Tiwari, R.P., et al., *Modern approaches to a rapid diagnosis of tuberculosis: promises and challenges ahead*. Tuberculosis, 2007. **87**(3): p. 193-201.
  53. Rogall, T., T. Flohr, and E.C. Böttger, *Differentiation of Mycobacterium species by direct sequencing of amplified DNA*. Journal of General Microbiology, 1990. **136**(9): p. 1915-1920.
  54. Park, H., et al., *Detection and identification of mycobacteria by amplification of the internal transcribed spacer regions with genus-and species-specific PCR primers*. Journal of Clinical Microbiology, 2000. **38**(11): p. 4080-4085.
  55. Hussain, M.M., T.M. Samir, and H.M. Azzazy, *Unmodified gold nanoparticles for direct and rapid detection of Mycobacterium tuberculosis complex*. Clinical Biochemistry, 2013. **46**(7): p. 633-637.
  56. Warren, R., et al., *Microevolution of the direct repeat region of Mycobacterium tuberculosis: implications for interpretation of spoligotyping data*. Journal of Clinical Microbiology, 2002. **40**(12): p. 4457-4465.
  57. Azzazy, H.M. and M.M. Mansour, *In vitro diagnostic prospects of nanoparticles*. Clinica Chimica Acta, 2009. **403**(1): p. 1-8.



58. Ray, P.C., et al., *Gold nanoparticle based FRET for DNA detection*. Plasmonics, 2007. **2**(4): p. 173-183.
59. Ray, P.C., A. Fortner, and G.K. Darbha, *Gold nanoparticle based FRET assay for the detection of DNA cleavage*. The Journal of Physical Chemistry B, 2006. **110**(42): p. 20745-20748.
60. Ghosh, D. and N. Chattopadhyay, *Gold nanoparticles: acceptors for efficient energy transfer from the photoexcited fluorophores*. Optics and Photonics Journal, 2013. **3**(01): p. 18-26.
61. Swierczewska, M., S. Lee, and X. Chen, *The design and application of fluorophore-gold nanoparticle activatable probes*. Physical Chemistry Chemical Physics, 2011. **13**(21): p. 9929-9941.
62. Qin, D., et al., *Using fluorescent nanoparticles and SYBR Green I based two-color flow cytometry to determine Mycobacterium tuberculosis avoiding false positives*. Biosensors and Bioelectronics, 2008. **24**(4): p. 626-631.
63. Stryer, L., *Fluorescence energy transfer as a spectroscopic ruler*. Annual Review of Biochemistry, 1978. **47**(1): p. 819-846.
64. Borlak, J., et al., *Molecular diagnosis of a familial nonhemolytic hyperbilirubinemia (Gilbert's syndrome) in healthy subjects*. Hepatology, 2000. **32**(4): p. 792-795.
65. Bretagne, S. and J.-M. Costa, *Towards a nucleic acid-based diagnosis in clinical parasitology and mycology*. Clinica Chimica Acta, 2006. **363**(1): p. 221-228.
66. Espy, M.J., et al., *Diagnosis of herpes simplex virus infections in the clinical laboratory by LightCycler PCR*. Journal of Clinical Microbiology, 2000. **38**(2): p. 795-799.
67. Ju-Nam, Y. and J.R. Lead, *Manufactured nanoparticles: an overview of their chemistry, interactions and potential environmental implications*. Science of the Total Environment, 2008. **400**(1): p. 396-414.
68. Turkevich, J., P.C. Stevenson, and J. Hillier, *A study of the nucleation and growth processes in the synthesis of colloidal gold*. Discussions of the Faraday Society, 1951. **11**: p. 55-75.

69. Daniel, M.-C. and D. Astruc, *Gold nanoparticles: assembly, supramolecular chemistry, quantum-size-related properties, and applications toward biology, catalysis, and nanotechnology*. Chemical Reviews, 2004. **104**(1): p. 293-346.
70. Hill, H.D. and C.A. Mirkin, *The bio-barcode assay for the detection of protein and nucleic acid targets using DTT-induced ligand exchange*. Nature Protocols , 2006. **1**(1): p. 324.
71. Soo, P.-C., et al., *A simple gold nanoparticle probes assay for identification of Mycobacterium tuberculosis and Mycobacterium tuberculosis complex from clinical specimens*. Molecular and Cellular Probes, 2009. **23**(5): p. 240-246.
72. Baptista, P.V., et al., *Gold-nanoparticle-probe-based assay for rapid and direct detection of Mycobacterium tuberculosis DNA in clinical samples*. Clinical Chemistry, 2006. **52**(7): p. 1433-1434.
73. Costa, P., et al., *Gold nanoprobe assay for the identification of mycobacteria of the Mycobacterium tuberculosis complex*. Clinical Microbiology and Infection, 2010. **16**(9): p. 1464-1469.
74. Liandris, E., et al., *Direct detection of unamplified DNA from pathogenic mycobacteria using DNA-derivatized gold nanoparticles*. Journal of Microbiological Methods, 2009. **78**(3): p. 260-264.
75. Das, M., Sumana, G., & Malhotra, B. D. (2010). Zirconia based nucleic acid sensor for Mycobacterium tuberculosis detection. Applied Physics Letters, **96**(13), 133703-1.
76. Hwang, S.-H., et al., *Upconversion nanoparticle-based Förster resonance energy transfer for detecting the IS6110 sequence of Mycobacterium tuberculosis complex in sputum*. Biosensors and Bioelectronics, 2014. **53**: p. 112-116.
77. Shojaei, T.R., et al., *Development of sandwich-form biosensor to detect Mycobacterium tuberculosis complex in clinical sputum specimens*. Brazilian Journal of Infectious Diseases, 2014. **18**(6): p. 600-608.
78. Saribas, Z., et al., *Use of fluorescence resonance energy transfer for rapid detection of isoniazid resistance in Mycobacterium tuberculosis clinical isolates*. The International Journal of Tuberculosis and Lung Disease, 2005. **9**(2): p. 181-187.

79. El-Hajj, H.H., et al., *Detection of Rifampin Resistance in Mycobacterium tuberculosis in a Single Tube with Molecular Beacons*. Journal of Clinical Microbiology, 2001. **39**(11): p. 4131-4137.
80. Ekrami, A., et al., *Validity of bioconjugated silica nanoparticles in comparison with direct smear, culture, and polymerase chain reaction for detection of Mycobacterium tuberculosis in sputum specimens*. International Journal of Nanomedicine, 2011. **6**: p. 2729.
81. Chia, B.S., et al., *Use of multiplex allele-specific polymerase chain reaction (MAS-PCR) to detect multidrug-resistant tuberculosis in Panama*. Plos One. 2012. e40456
82. Mujumdar, R.B., et al., *Cyanine dye labeling reagents: sulfoindocyanine succinimidyl esters*. Bioconjugate Chemistry, 1993. **4**(2): p. 105-111.
83. Dulkeith, E., et al., *Fluorescence quenching of dye molecules near gold nanoparticles: radiative and nonradiative effects*. Physical Review Letters, 2002. **89**(20): p. 203002.
84. Telenti, A., *Genetics of drug resistant tuberculosis*. Thorax, 1998. **53**(9): p. 793-797.
85. Musser, J.M., *Antimicrobial agent resistance in mycobacteria: molecular genetic insights*. Clinical Microbiology Reviews, 1995. **8**(4): p. 496-514.
86. Ahmad, S. and E. Mokaddas, *Recent advances in the diagnosis and treatment of multidrug-resistant tuberculosis*. Respiratory Medicine, 2009. **103**(12): p. 1777-1790.
87. Abbadi, S.H., et al., *Molecular identification of mutations associated with anti-tuberculosis drug resistance among strains of Mycobacterium tuberculosis*. International Journal of Infectious Diseases, 2009. **13**(6): p. 673-678.
88. Bloemberg, G.V., et al., *Evaluation of Cobas TaqMan MTB for direct detection of the Mycobacterium tuberculosis complex in comparison with Cobas Amplicor MTB*. Journal of Clinical Microbiology, 2013. **51**(7): p. 2112-2117.
89. Yang, Y.-C., et al., *Evaluation of the Cobas TaqMan MTB test for direct detection of Mycobacterium tuberculosis complex in respiratory specimens*. Journal of Clinical Microbiology, 2011. **49**(3): p. 797-801.

90. Palomino, J.C., *Molecular detection, identification and drug resistance detection in Mycobacterium tuberculosis*. FEMS Immunology & Medical Microbiology, 2009. **56**(2): p. 103-111.
91. Bergmann, J.S. and G.L. Woods, *Clinical evaluation of the Roche AMPLICOR PCR Mycobacterium tuberculosis test for detection of M. tuberculosis in respiratory specimens*. Journal of Clinical Microbiology, 1996. **34**(5): p. 1083-1085.
92. Drobniewski, F., et al., *Modern laboratory diagnosis of tuberculosis*. The Lancet Infectious Diseases, 2003. **3**(3): p. 141-147.
93. Iwamoto, T., T. Sonobe, and K. Hayashi, *Loop-mediated isothermal amplification for direct detection of Mycobacterium tuberculosis complex, M. avium, and M. intracellulare in sputum samples*. Journal of Clinical Microbiology, 2003. **41**(6): p. 2616-2622.
94. Hillemann, D., et al., *Rapid molecular detection of extrapulmonary tuberculosis by the automated GeneXpert MTB/RIF system*. Journal of Clinical Microbiology, 2011. **49**(4): p. 1202-1205.
95. Kim, C.K., et al., *Gold-nanoparticle-based miniaturized laser-induced fluorescence probe for specific DNA hybridization detection: studies on size-dependent optical properties*. Nanotechnology, 2006. **17**(13): p. 3085.
96. Boehme, C.C., et al., *Rapid molecular detection of tuberculosis and rifampin resistance*. New England Journal of Medicine, 2010. **363**(11): p. 1005-1015.
97. Chedore, P. and F. Jamieson, *Rapid molecular diagnosis of tuberculous meningitis using the Gen-probe Amplified Mycobacterium Tuberculosis direct test in a large Canadian public health laboratory*. The International Journal of Tuberculosis and Lung Disease, 2002. **6**(10): p. 913-919.
98. Soini, H. and J.M. Musser, *Molecular diagnosis of mycobacteria*. Clinical Chemistry, 2001. **47**(5): p. 809-814.
99. Garg, S.K., et al., *Diagnosis of tuberculosis: available technologies, limitations, and possibilities*. Journal of Clinical Laboratory Analysis, 2003. **17**(5): p. 155-163.
100. Roth, A., T. Schaberg, and H. Mauch, *Molecular diagnosis of tuberculosis: current clinical validity and future perspectives*. European Respiratory Journal, 1997. **10**(8): p. 1877-1891.

101. Motré, A., R. Kong, and Y. Li, *Improving isothermal DNA amplification speed for the rapid detection of Mycobacterium tuberculosis*. *Journal of Microbiological Methods*, 2011. **84**(2): p. 343-345.